

Design, Synthesis, and Biological Evaluation of Novel Fluorescent Probes Targeting the 18-kDa Translocator Protein

Hendris Wongso,^{*,[a, b]} Tomoteru Yamasaki,^[c] Katsushi Kumata,^[c] Maiko Ono,^[d] Makoto Higuchi,^[d] Ming-Rong Zhang,^[c] Michael J. Fulham,^[e] Andrew Katsifis,^{*,[e]} and Paul A. Keller^{*,[a]}

A series of fluorescent probes from the 6-chloro-2-phenylimidazo[1,2-*a*]pyridine-3-yl acetamides ligands featuring the 7-nitro-2-oxa-1,3-diazol-4-yl (NBD) moiety has been synthesized and biologically evaluated for their fluorescence properties and for their binding affinity to the 18-kDa translocator protein (TSPO). Spectroscopic studies including UV/Vis absorption and fluorescence measurements showed that the synthesized fluorescent probes exhibit favorable spectroscopic properties, especially in nonpolar environments. *In vitro* fluorescence staining in brain sections from lipopolysaccharide (LPS)-injected

mice revealed partial colocalization of the probes with the TSPO. The TSPO binding affinity of the probes was measured on crude mitochondrial fractions separated from rat brain homogenates in a [¹¹C]PK11195 radioligand binding assay. All the new fluorescent probes demonstrated moderate to high binding affinity to the TSPO, with affinity (K_i) values ranging from 0.58 nM to 3.28 μ M. Taking these data together, we propose that the new fluorescent probes could be used to visualize the TSPO.

Introduction

The 18-kDa translocator protein (TSPO) is part of a five transmembrane hetero-oligomeric complex widely expressed in peripheral organs such as the heart, kidney, lungs, and steroid-producing tissues and in lower concentrations in the central nervous system (CNS).^[1,2] In the CNS, TSPO is involved in neurosteroid synthesis, regulation of mitochondrial function, and modulation of neuroinflammation in microglial cells and astrocytes. Importantly, TSPO expression is markedly upregulated in activated microglia and reactive astrocytes in response

to inflammatory stimuli or brain injury.^[3,4] It is therefore considered an important and sensitive marker of microglial-astrocyte activation and inflammation. In addition to its overexpression in neurodegenerative diseases, an increase in the expression of the TSPO has also been seen in atherosclerosis, stroke, arthritis, cardiovascular disease^[5] and several cancers including brain,^[6] prostate,^[7] colon,^[8] and breast.^[9] Furthermore, it is reported that TSPO expression correlated positively with disease progression whilst the prognosis of some cancers correlate negatively with the expression of TSPO.^[10] Therefore numerous studies involving TSPO radioligands have been investigated as a means of monitoring neuroinflammation, neurodegeneration, cancer and cardiovascular disease in pre-clinical and clinical studies using the imaging modalities positron emission tomography (PET) and single photon emission computed tomography (SPECT).^[11,12]

To date, radioligands targeting TSPO, exemplified by the isoquinoline carboxamide ([¹¹C]PK11195),^[13] imidazo[1,2-*a*]pyridine ([¹⁸F]PBR111),^[14] 2-aryl-8-oxodihydropurine acetamide ([¹⁸F]FEDAC),^[15] phenoxyarylacacetamide ([¹⁸F]DAA1106),^[16] arylox-yaniide ([¹¹C]PBR28),^[17] and the tricyclic indole ([¹⁸F]GE180)^[18] (Figure 1) have been prepared and evaluated preclinically and clinically.

In parallel, fluorescence/optical imaging, has been widely used in *in vitro* histologic examination of cells and tissue, and in *in vivo* imaging studies using small animals. However, due to photon scattering and light attenuation by biological tissue, fluorescence imaging is limited by depth penetration and is unable to provide *in vivo* quantitative or tomographic information in large animals or human subjects.^[19] More recently, fluorescence imaging has gained considerable interest in improving surgical interventions. As a result, clinical studies that

[a] Dr. H. Wongso, Prof. P. A. Keller
School of Chemistry and Molecular Bioscience, and Molecular Horizons
University of Wollongong
Wollongong, NSW 2522 (Australia)
E-mail: keller@uow.edu.au
hw765@uowmail.edu.au

[b] Dr. H. Wongso
Center for Applied Nuclear Science and Technology
National Nuclear Energy Agency
Bandung 40132 (Indonesia)

[c] Dr. T. Yamasaki, Dr. K. Kumata, Prof. M.-R. Zhang
Department of Advanced Nuclear Medicine Sciences
National Institute of Radiological Sciences
Chiba 263-8555 (Japan)

[d] Prof. M. Ono, Prof. M. Higuchi
Department of Functional Brain Imaging Research
National Institutes for Quantum and Radiological Science and Technology
Chiba 263-8555 (Japan)

[e] Prof. M. J. Fulham, Prof. A. Katsifis
Department of PET and Nuclear Medicine
Royal Prince Alfred Hospital
Camperdown, NSW 2050 (Australia)
E-mail: andrewk@nucmed.rpa.cs.nsw.gov.au

 Supporting information for this article is available on the WWW under <https://doi.org/10.1002/cmdc.202000984>

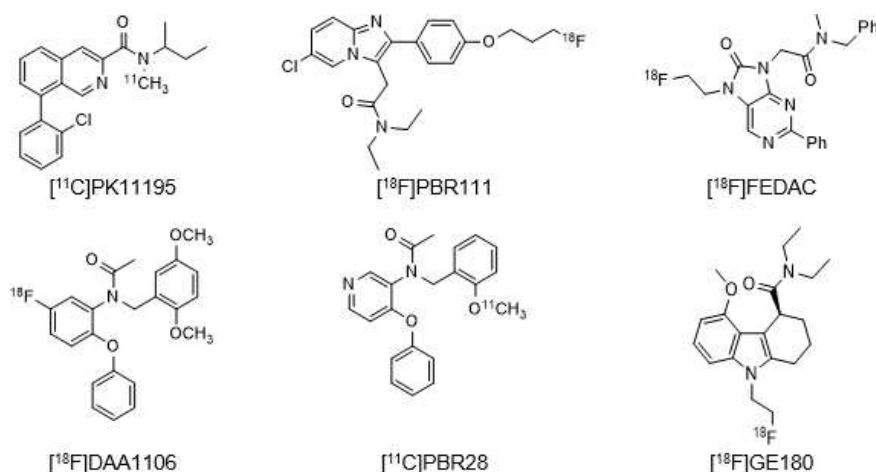


Figure 1. Structures of several radiolabeled TSPO ligands.

combined the clinical utility of PET-CT and fluorescence imaging for improving tumor excision, reduced local recurrence and for improving patient prognosis have been investigated.^[20,21] Hence, the conjugation of various fluorophores to TSPO ligands to produce TSPO fluorescent probes offers considerable opportunities in biological and clinical studies to complement the use of radioligands.

The development of high-affinity and selective fluorescent or dual-modality PET fluorescent imaging agents based on small drug-like molecules has been synthetically challenging due to the relatively large size of the fluorescent moiety, and the steric impact these structures have on the binding to the receptor. Furthermore, the type of fluorophore, and the mode of attachment not only impacts affinity and selectivity, but also biodistribution, uptake and clearance of the imaging agent *in vivo*.^[22] A common approach to developing fluorescent probes has been the attachment of the fluorophore to the parent ligand through the use of linkers to minimize interference between the binding domain of the targeting ligand and the biological target.^[23] It is also well recognized that the length and types of linkers have an enormous influence on the ligand's binding affinity, selectivity, and the pharmacokinetic and pharmacodynamic properties *in vivo*.^[24,25] The structures of several fluorescent TSPO probes developed for the visualization of activated microglia by fluorescence microscopy are shown in Figure 2.

Recently, several TSPO ligands have been exploited as fluorescent/near infrared probes for imaging the TSPO *in vitro* and *in vivo*.^[27,28,31,32] Literature data and our own results suggest that 6-chloro-2-phenylimidazo[1,2-a]pyridine-3-yl acetamides of general structure 1 (Figure 3) exhibit high affinity for the TSPO, when R₁ and R₂ are small alkyl groups whilst the *para* position 'X' on the 2-phenyl ring is able to tolerate relatively large groups.^[33] Thus, it was hypothesized that X, R¹ and R² substituents can be used to attach fluorophores using suitable linkers. Therefore, the derivatisation of the imidazopyridine is consistent with a previously reported study involving the attachment of the fluorescent NBD moiety with various sized

linkers on the acetamide side chain of the imidazopyridine skeleton which showed moderate affinity for the TSPO.^[25]

The aims of this project were to develop high affinity and selective TSPO fluorescent ligands based on the imidazopyridine chemical structure suitable for *in vitro*, *ex vivo* and *in vivo* applications. To this end, this work investigated the attachment of the fluorophore both on the acetamide side chain (fluorophore attachment I) and on the 2-(4'-phenyl) (fluorophore attachment II) of the 2-phenylimidazo[1,2-a]pyridine-3-yl acetamide and their preliminary biological evaluation. The probe incorporated was the simple and relatively small 7-nitro-2-oxa-1,3-diazole using different sized linkers to study the effect of these substituents on TSPO binding, the outcomes of which could be used later to develop other fluorescent probes with emissions suitable for *in vitro*, *ex vivo* or *in vivo* applications. Herein, we report and discuss the synthesis and biological evaluation of these novel imidazopyridine fluorescent probes for potential use in visualizing the TSPO.

Results and Discussion

We have previously identified highly potent and selective TSPO ligands based on the imidazo[1,2-a]pyridines, pyrazolopyrimidine structures, which were developed as PET ligands radiolabeled with ¹⁸F (Figure 4).^[34] This current study investigated TSPO-fluorescent probes generated from the conjugation of TSPO ligand 2 with the commercially available fluorophore, NBD, selected as it has been previously investigated as a fluorophore for spectroscopic and microscopic applications in biophysical, biochemical, and cell biological studies.^[35,36] NBD-containing ligands typically exhibit a low quantum yield in aqueous solution and protic environments, but are highly fluorescent in a nonpolar medium or when bound to membranes or hydrophobic residues in protein pockets. A further advantage is its relatively small size compared to other probes, which may have less impact on the affinity and

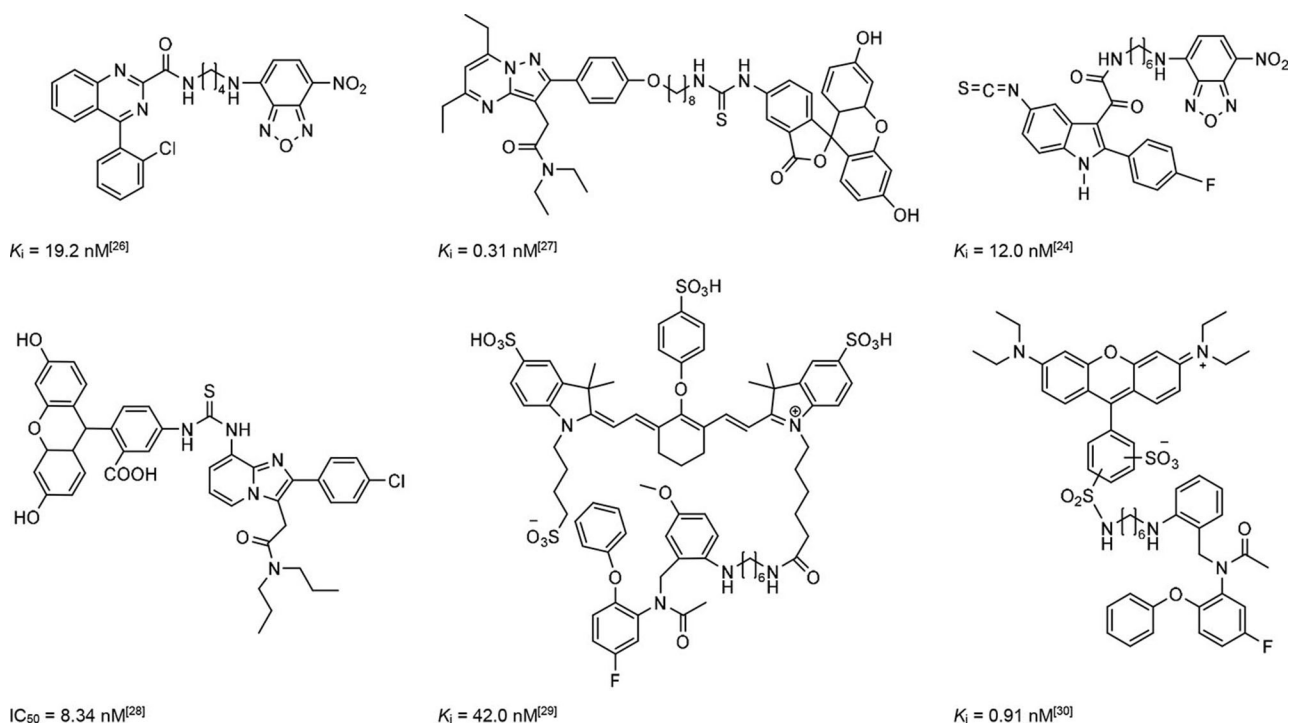


Figure 2. Structure of several TSPO fluorescent probes.

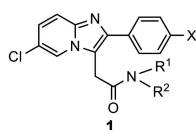


Figure 3. General structure of imidazo[1,2-a]pyridine TSPO ligands.

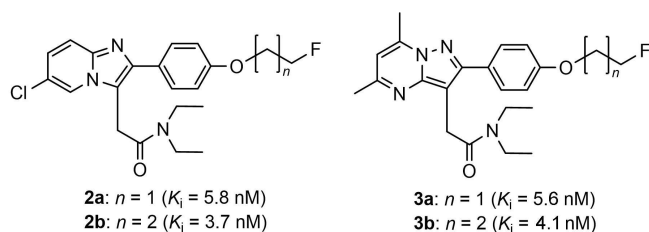


Figure 4. Two examples of PET TSPO ligands radiolabeled with fluorine-18.

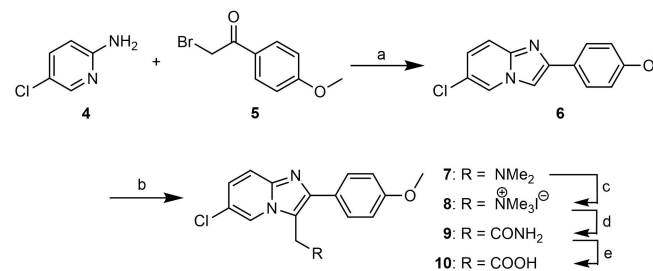
selectivity of the parent ligand during ligand development stages.^[24]

Chemistry

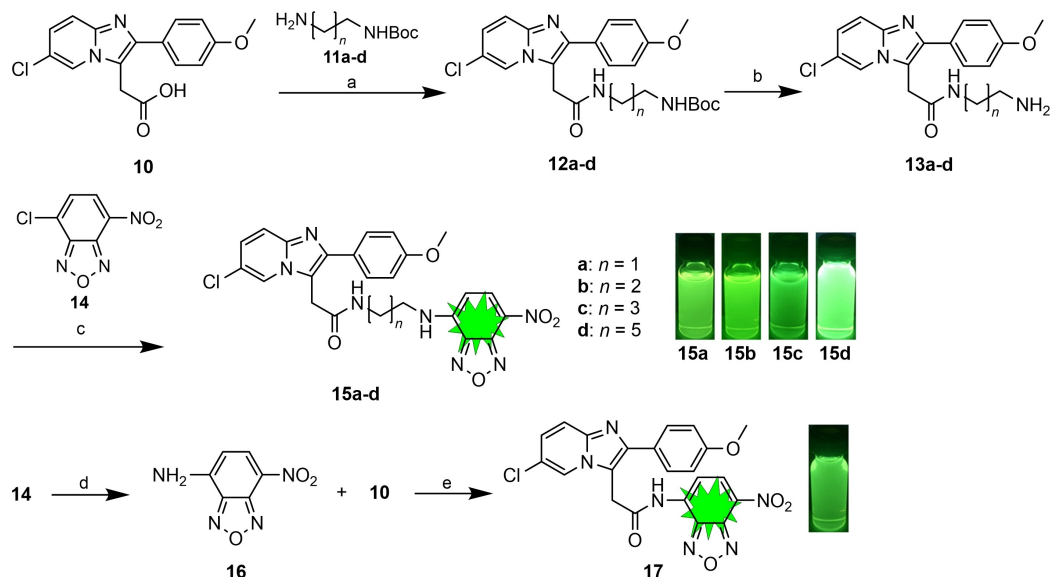
The synthesis of imidazopyridineacetic acid **10** started with a standard condensation of commercially available 5-chloropyridin-2-amine **4** and 2-bromo-4'-methoxyacetophenone **5** in ethanol at reflux to produce imidazopyridine **6** in 73%, which subsequently underwent a Mannich condensation with aqueous formaldehyde (H_2CO) and dimethylamine ($\text{NH}(\text{CH}_3)_2$) in acetic

acid (AcOH) to give tertiary amine **7** in 69%, followed by quaternization with methyl iodide (CH_3I) at room temperature to produce the ammonium iodide **8** in 84%. The desired acetamide **9** was obtained in 71% yield upon treatment with KCN, followed by hydrolysis under strongly alkaline conditions (KOH in ethanol) and gave the corresponding imidazopyridineacetic acid **10** in 94% yield (Scheme 1).

The imidazopyridineacetic acid **10** then entered divergent synthesis pathways to generate probes with the attachment of the fluorophore moiety at the 3-acetamide side chain (path A, fluorophore attachment I) or on the phenyl ring of the imidazopyridine structure (path B, fluorophore attachment II). The synthesis of fluorescent probes **15a–d** (path A; Scheme 2) involved the peptide coupling of the acid **10** with the appropriate mono-Boc-protected polymethylenediamine **11a–d** in the presence of HOBt, EDCI, and DIPEA generating amides



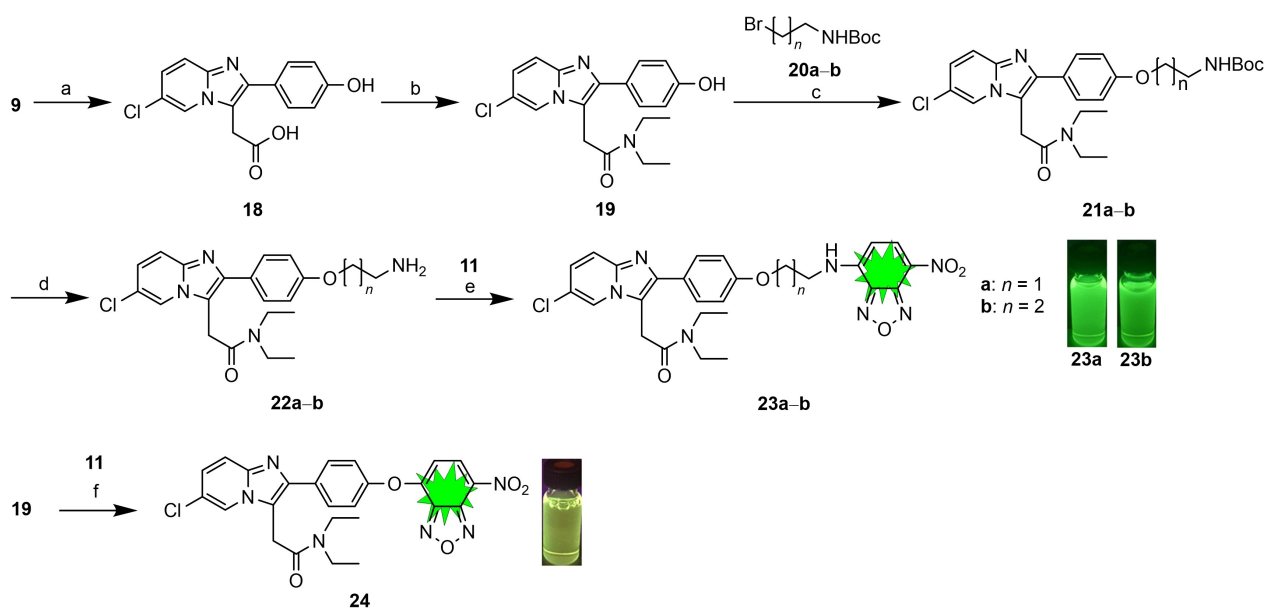
Scheme 1. a) NaHCO_3 , EtOH, reflux, 10.5 h, 73%; b) $(\text{CH}_3)_2\text{NH}$ (aq), CH_2O , CH_3COOH , 55°C , 18 h, 69%; c) CH_3I , toluene, RT, 48 h, darkness, 84%; d) KCN, EtOH, H_2O , reflux, 48 h, 71%; e) KOH, EtOH, H_2O , reflux, 18 h, 94%.



Scheme 2. a) HOBt, EDCl, DIPEA, DMF, RT, 24 h, 74–96%; b) $\text{CF}_3\text{CO}_2\text{H}$, CH_2Cl_2 , RT, 4 h, 85–89%; c) DIPEA, DMF, 0°C – RT, 18 h, darkness, 42–57%; d) NH_4OH , MeOH, 0°C – RT, 18 h, darkness, 51%; e) HOBt, EDCl, DIPEA, DMF, RT, 48 h, 62%. **15a–d**, **17**: fluorescent probes in MeOH ($\sim 1.0\%$, w/v) upon UV irradiation ($\lambda = 365$ nm).

12a–d in 74–96% yields. Boc deprotection with $\text{CF}_3\text{CO}_2\text{H}$ (TFA) produced free amines **13a–d** in 85–89% yields. Condensation of amines **13a–d** with NBD–Cl **14** in the presence of DIPEA to give the desired probes **15a–d** in moderate yields (42–57%). NBD–amine **16** was obtained in 51% yield from the treatment of NBD–Cl **14** with NH_4OH in methanol. Synthesis of probe **17** was achieved from direct conjugation of NBD–amine **16** with imidazopyridineacetic acid **10** in 62% yield, using a similar procedure for **12a–d**.

The synthesis of probes **23a–b** (Path B) was accomplished in a five-step procedure (Scheme 3), starting with demethylation and hydrolysis of acetamide **9** using HBr in acetic acid to afford the corresponding carboxylic acid **18** in 63% yield. The amide **19** was realized in 74% yield by peptide coupling of the acid **18** with diethylamine in the presence of HOBt, EDCl, DIPEA in anhydrous DMF. Alkylation of the phenol group with the appropriate Boc-protected bromoamine **20a–b**, produced *O*-alkylated derivatives **21a–b** in 71–72% yields. Further treatment



Scheme 3. a) HBr, CH_3COOH , 110°C , 48 h, 63%; b) DEA, HOBt, EDCl, DIPEA, DMF, RT, 24 h, 74%; c) K_2CO_3 , DMF, RT, 48 h, 71–72%; d) $\text{CF}_3\text{CO}_2\text{H}$, CH_2Cl_2 , RT, 4 h, 88–92%; e) DIPEA, DMF, 0°C – RT, 18 h, darkness, 42–44%; f) DIPEA, DMF, 0°C – RT, 18 h, darkness, 43%. **23a–b**, **24**: fluorescent probes **23a–b**, **24** in MeOH ($\sim 1.0\%$ (w/v)) upon UV irradiation ($\lambda = 365$ nm).

with $\text{CF}_3\text{CO}_2\text{H}$ in CH_2Cl_2 afforded the free amines **22 a–b** in 88–92% yields. The synthesis of fluorescent compounds **23 a–b** was completed by conjugation of amines **22 a–b** with NBD-Cl **14** in the presence of DIPEA in 42–44% yields. Synthesis of probe **24** was achieved in 43% yield *via* direct conjugation of phenol **19** with NBD-Cl **14** in the presence of DIPEA in anhydrous DMF. (Scheme 3).

Spectroscopic properties of fluorescent probes **23 a**, **23 b** and **24**

The ultraviolet absorption (Figure 5) and the fluorescence properties (Figure 6) of the selected fluorescent compounds **23 a**, **23 b** and **24** were investigated in different environments. These probes were selected for spectroscopic studies as they showed excellent binding affinity for the TSPO (Table 3). As the first step, compounds were dissolved in dimethyl sulfoxide

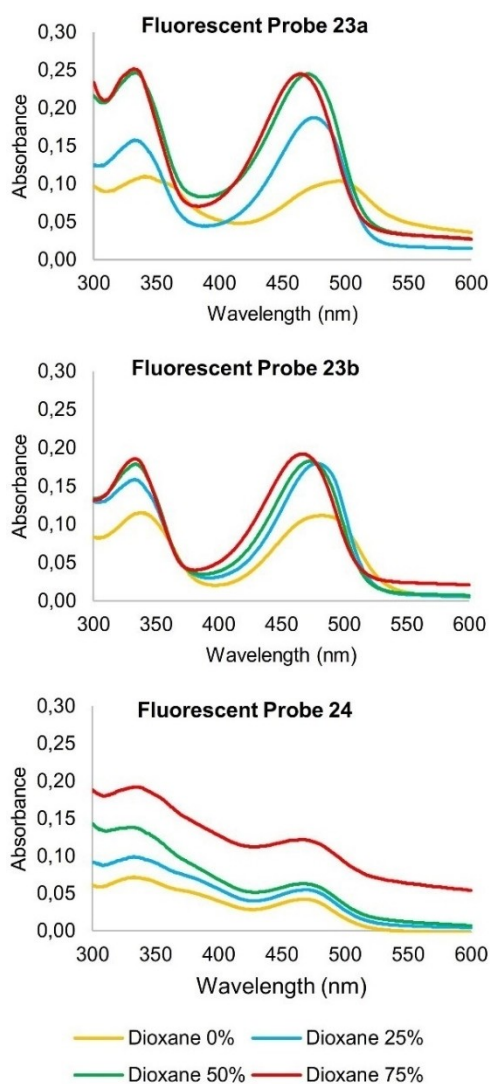


Figure 5. Ultraviolet absorption spectra of compounds **23 a**, **23 b**, and **24** at $10\ \mu\text{M}$ in solutions varying from 0 to 75% *v/v* dioxane in PBS.

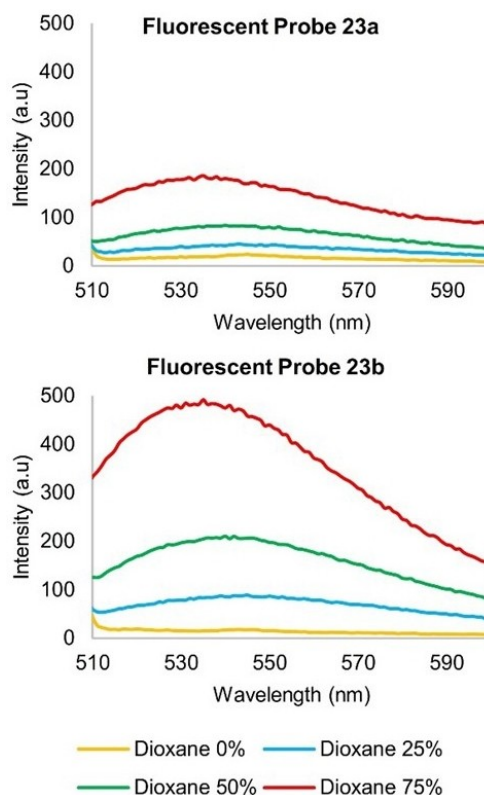


Figure 6. Effect of the polarity of the medium on the fluorescence of compounds **23 a** and **23 b** at $10\ \mu\text{M}$ in solutions varying from 0 to 75% *v/v* dioxane in PBS.

(DMSO), diluted to a final concentration of $10\ \mu\text{M}$ in different assay solutions from 0% dioxane to 75% *v/v* dioxane/water phosphate-buffered saline (PBS). The percentage of DMSO used in the assay did not exceed 1% of the final volume solution. In aqueous solution (0% *v/v* dioxane/PBS), the spectrum of probe **23 a** is characterized by two absorptions maxima at 340 and 490 nm, showing extinction coefficients of $\epsilon = 11\,000$ and $10\,400\ \text{M}^{-1}\text{cm}^{-1}$, respectively. When probe **23 a** was dissolved in 25% *v/v* dioxane/PBS, the spectrum is characterized by two absorption maxima at 330 and 470 nm, and the increase of the extinction coefficients ($\epsilon = 15\,800$ and $18\,700\ \text{M}^{-1}\text{cm}^{-1}$, respectively). A further increase in hydrophobicity of the medium (50% *v/v* dioxane/PBS) caused an increase of the extinction coefficients to $24\,700\ \text{M}^{-1}\text{cm}^{-1}$ and $24\,500\ \text{M}^{-1}\text{cm}^{-1}$, respectively. In the PBS solution containing 75% dioxane (*v/v*), the extinction coefficients remained almost constant.

Fluorescence staining

To confirm the probe binding to TSPO expressed with inflammation, *in vitro* fluorescence staining using brain sections from lipopolysaccharide (LPS)-injected mice^[38] was carried out. In this study, $4\ \mu\text{g}$ of LPS was injected into the striatum of the right hemisphere, and the induction of TSPO

expression with LPS injection was confirmed by immunostaining with anti-TSPO antibody (Table 1). Double staining of brain sections from LPS-injected mice with probes as well as anti-TSPO antibody illustrated that the green signals derived from the tested probes and red signals derived from anti-TSPO antibody were partially colocalized in several probes, including **15a–d** and **23a–b** (Table 2). These data suggested that the binding activity of probes to TSPO in the tissue slices of mouse brain evoked an inflammation under the environment where high concentrations of probe (17.3–19.2 μM) can react with TSPO.

The absorption spectra of probe **23b** show a similar profile to that of probe **23a**, suggesting that higher hydrophobicity of the medium can promote the increase of the extinction coefficient. From this probe, the highest extinction coefficient ($\epsilon = 19200 \text{ M}^{-1} \text{ cm}^{-1}$) was observed in 75% v/v dioxane/PBS solution at 470 nm. The absorptions maxima of probe **24** was generally lower compared to both probes **23a** and **23b**, with the spectra characterized by two absorptions maxima at 330 and 470 nm, and the highest extinction coefficient ($\epsilon = 19200 \text{ M}^{-1} \text{ cm}^{-1}$) was observed at 470 nm in the PBS solution containing 75% dioxane (v/v).

Table 1. Fluorescent images of brain sections from LPS-injected mice stained with anti-TSPO antibody.

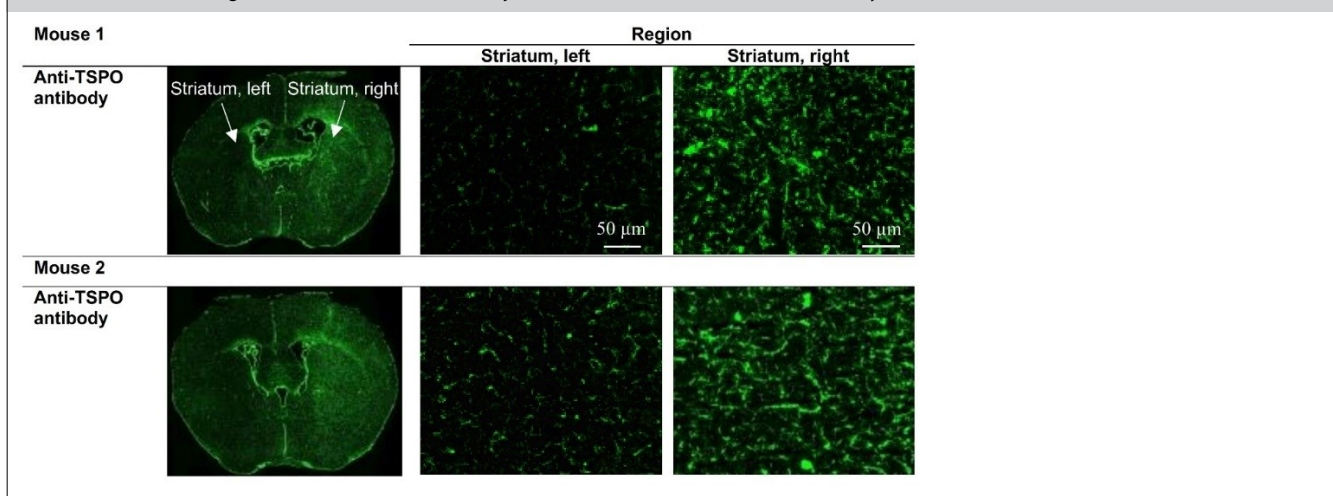
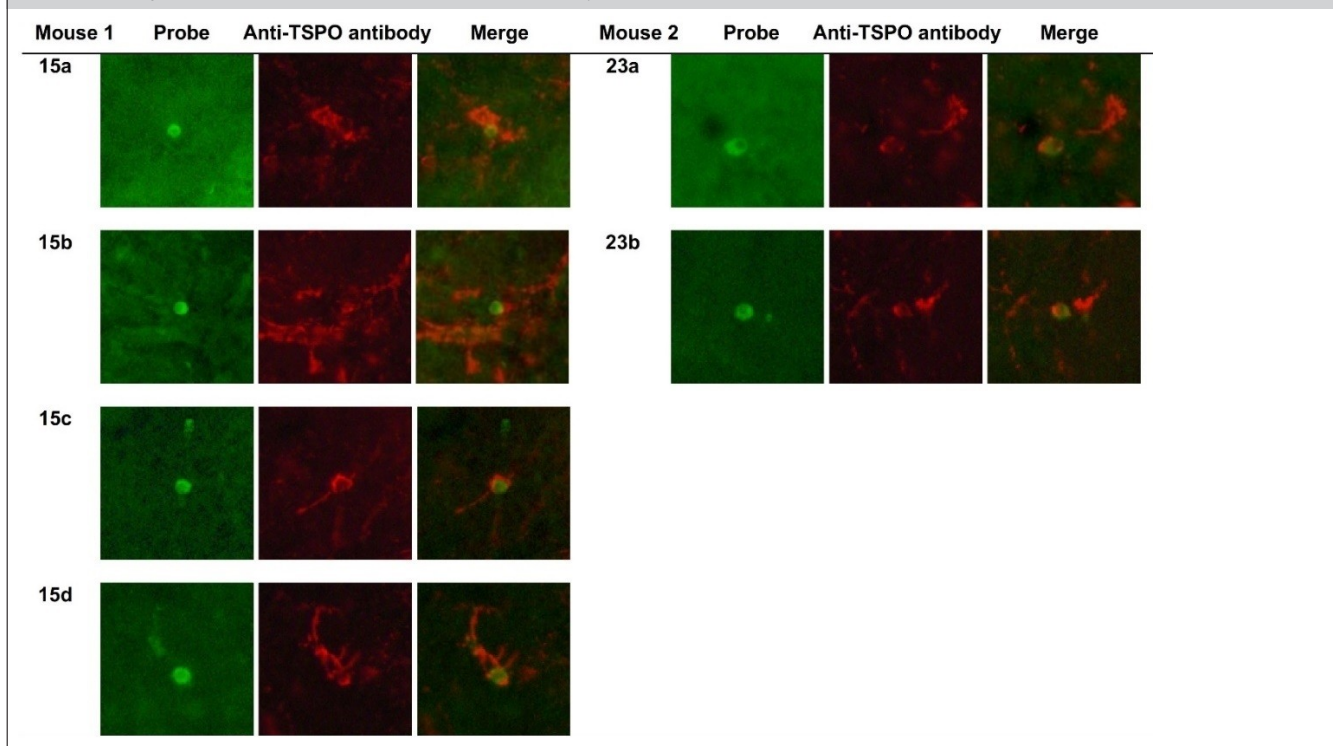


Table 2. Binding of probes to TSPO in the brain section from LPS-injected mouse.



Probes **23a** and **23b** displayed emission maxima at 535 nm, which correspond to the NBD moiety emission (Figure 6). Interestingly, probe **23b** with the longer carbon linker ($n=2$) showed a significant increase of fluorescence intensity compared to probe **23a** ($n=1$). Additionally, decreasing the polarity of the medium (from 0 to 75% v/v dioxane in PBS) promoted an approximately tenfold and 32-fold increase in the fluorescence intensity of probes **23a** and **23b**, respectively. This suggests that NBD-containing compounds exhibits a high degree of environmental sensitivity.^[36] In contrast, probe **24** without any carbon methylene linker between the parent ligand and NBD demonstrated a very low fluorescence intensity at 500 to 600 nm, probably due to intramolecular fluorescence quenching.^[37] However, an increase in fluorescence intensity was observed at 410 nm (see Figure S73 in the Supporting Information).

TSPO binding affinity

The affinity of the newly synthesized compounds for the TSPO was determined in a competitive binding assay using crude mitochondrial fraction, centrifuged from rat brain homogenates with [¹¹C]PK11195 as the competitive radioligand. With PK11195 as the reference standard, the fluorescent probes showed moderate to high affinity binding to the TSPO, with K_i values ranging from 0.58 nM for compound **23b** and 3.28 μ M for **15d** (Table 3)

Overall, fluorescent compounds with the attachment of the NBDs at the 3-acetamide side chain (Path A, fluorophore attachment I) showed lower affinity for the TSPO ($K_i=242.43$ – 3276.30 nM) compared to probes with the attachment of the NBDs on the 4'-position of the 2-phenyl ring of the imidazopyridine structure (Path B, fluorophore attachment II; $K_i=0.58$ – 1.44 nM). Probes **15a–d** with carbon linker varying from 2 to 6, generally showed low to moderate affinity for the TSPO. In this subset, significant improvement in affinity was observed by reducing the length of the linkers. Additionally, compound **17**, which represents the fluorescent compound without a carbon linker demonstrated higher affinity than probes **15a–d** which showed progressive reduction in affinity

Table 3. TSPO binding affinity of the fluorescent probes.

Fluorescent probe	IC ₅₀ [μ M]	K_i [nM]
15a	7.09 \pm 0.03	242.43 \pm 28.85
15b	34.87 \pm 5.45	1205.57 \pm 334.28
15c	84.13 \pm 7.66	2896.57 \pm 619.05
15d	100.50 \pm 74.15	3276.30 \pm 2111.83
17	2.28 \pm 0.44	76.91 \pm 5.51
23a	0.01 \pm 0.01	1.35 \pm 0.70
23b	0.005 \pm 0.00	0.58 \pm 0.12
24	0.04 \pm 0.00	1.44 \pm 0.13
PK11195	0.008 \pm 0.00	0.59 \pm 0.20

The concentration of tested probes that inhibited [¹¹C]PK11195 binding at rat brain mitochondrial membranes (IC₅₀) by 50% was determined with six concentrations of the displacers, each performed in duplicate. The IC₅₀ values were converted to an absolute constant K_i using the Cheng-Prusoff equation.

with increasing carbon linker length. The moderate binding affinity of these probes bearing the NBD substituents on the acetamide side chain of the imidazopyridine is consistent with those reported by previous investigators.^[25] On the other hand, the attachment of the NBDs on the *para*-position of the phenyl ring of the ligand resulted in an excellent binding affinity as exemplified by probes **23a** ($K_i=1.35$ nM), **23b** ($K_i=0.58$ nM) and **24** ($K_i=1.44$ nM), confirming our previous studies that this position of the 2-phenylimidazopyridine group was more tolerant of large functional groups in maintaining affinity for the TSPO receptor. The fluorescent compound bearing a C₂ linker (**23b**) exhibited the highest binding affinity ($K_i=0.58$ nM), which was twice as high as compounds **23a** and **24**, respectively. To the best of our knowledge, compound **23b** is the highest affinity fluorescent probe among the NBD-based TSPO fluorescent probes that have been reported. More interestingly, the affinity of this compound is 6–10 times higher than its parent ligand analogues (**2a–b**), indicating that the introduction of the fluorophore may not always decrease the affinity of the parent ligand. Although the binding affinity of these probes to the central benzodiazepine receptor (CBR) were not determined, the *in vitro* studies with these probes in LPS-lesioned mice shows colocalization with anti-TSPO antibody in lesions, suggesting selectivity for the TSPO over the CBR. Further ligand optimization and their specificity and selectivity for the TSPO over CBR and other targets will be conducted.

Conclusion

A series of novel fluorescent probes based on the 6-chloro-2-phenylimidazo[1,2-*a*]pyridine-3-yl acetamide structure has been developed, bearing the 7-nitro-2-oxa-1,3-diazol-4-yl (NBD) moiety on the 2-(4'-phenyl) position as well as on the 3-acetamide side chain. All of the new fluorescent probes demonstrated moderate to high binding affinity (K_i) values for the TSPO, with nanomolar binding of ligands bearing the NBD in the 2-(4'-phenyl) position compared to micromolar affinity for those on the 3-acetamide side chain.

Experimental Section

General chemistry

Unless stated otherwise, all chemicals were laboratory or reagent grade and were purchased from Merck (Australia) or AK Scientific, Inc (USA). All chemicals were used as received. All solvents were reagent grade and, when necessary, were purified and dried by standard methods. Water was purified *via* Millipore filtration prior to use. HOBt was purchased with added stabilizer (10% w/w H₂O), and therefore, the quantity required for reactions was adjusted accordingly and is reflected in the reagent mass reported in the experimental. All reactions requiring anhydrous conditions were conducted under a positive atmosphere of nitrogen in oven-dried glassware. Cold reaction temperatures were obtained by an ice bath (0 °C). Heating of reaction was performed with a paraffin oil bath. Standard syringe and autopipette techniques were used for

the anhydrous addition of liquids. Reactions were routinely monitored by TLC analysis performed on aluminium-backed SiO₂ gel plates (F254 grade – 0.20 mm thickness) or by low resolution mass spectrometry (LRMS) on Shimadzu LC-2010 mass spectrometer. Visualization on TLC plates was achieved with UV light ($\lambda = 254, 365$ nm), ninhydrin stain, or cerium ammonium molybdate stain. All filtrations were conducted as a gravity filtration through a filter paper Whatman Grade 4 (20–25 μm) or as a vacuum filtration through a sintered glass funnel (medium porosity). Vacuum filtration was achieved with the aid of vacuum pump. Organic solutions were dried over anhydrous Na₂SO₄. Solvent removal *via* concentration was performed on a rotary evaporator under reduced pressure. All solvent mixtures are expressed in terms of volume ratio (i.e., v/v). Normal phase flash column chromatography was performed on SiO₂ gel 60 with a positive air pressure. Preparative TLC was run using PLC silica gel 60 F₂₅₄ 1 mm plates (20×20 cm²). All synthesized compounds were dried under high vacuum (<1 mbar) before determination of chemical yields and spectroscopic characterization. All synthesized compounds were subjected to full spectroscopic characterization and assignment. Melting points were determined on a Gallenkamp melting point apparatus in open capillary tubes and were uncorrected. ¹H and ¹³C NMR spectra were recorded on a Bruker Avance 400 (400 MHz) or Varian Inova 500 (500 MHz) NMR spectrometer. Chemical shifts (δ) were reported in parts per million (ppm) relative to the internal standard. Samples were dissolved in CDCl₃ (with TMS as the internal standard – 0.00 ppm), CD₃OD (solvent resonance as internal standard – 3.31 ppm) or [D₆]DMSO (solvent resonance as internal standard – 2.50 ppm). ¹³C NMR signal assignments were confirmed by analysis of NMR experiments: APT, gCOSY, gHSQC, gHMBC, zTOCSY, NOESY and/or gHSQC-TOCSY. Low resolution mass spectrometry (LRMS) spectra were recorded on a Shimadzu LC-2010 mass spectrometer in electrospray positive and negative ionization modes (ESI-MS). High resolution mass spectrometry (HRMS) spectra were recorded on a Waters Quadrupole-Time of Flight (QTOF) Xevo or Thermo LTQ Orbitrap XL 158 spectrometer in electrospray positive and negative ionization modes (ESI-MS). All mass spectrometry samples were dissolved in HPLC grade MeOH. Solid-state infrared spectroscopy was performed on a Bruker Vertex 70 FTIR spectrometer in combination with a MIRAcle 10 Single Reflection Attenuated Total Reflectance accessory outfitted with a 1.5 mm round diamond crystal. IR peaks are reported as the wavenumber (ν_{max} in cm⁻¹) of the maximum absorption. Ultraviolet absorption spectra were recorded on a Shimadzu 1800 spectrometer. Fluorescence spectra were recorded on a Cary Eclipse fluorescence spectrophotometer with a slit width of 5 mm used for both excitation and emission. Ultraviolet absorption and fluorescence spectra were recorded at ambient temperature (23 ± 2 °C). Compounds were prepared as stock solutions in DMSO and diluted such that the DMSO concentration did not exceed 1% v/v. Analytical HPLC was performed on a Shimadzu LC-2030 C 3D UV/Vis detector ($\lambda = 254$ nm) using a biphenyl column Kinetex 100 Å (150×4.60 mm; 5 μm) at 25 °C using mobile phases A (water and 0.1% trifluoroacetic acid (TFA)) and B (MeCN and 0.1% TFA) at a flow rate of 1 mL min⁻¹. The following gradient was applied: gradient elution for 35 min at 0–50% of solvent B, linear increase from 0%–50% of solvent B over 25 min, hold at 50% of solvent B for 10 min. The purity of all final compounds was found to be higher than 95%.

6-Chloro-2-(4-methoxyphenyl)imidazo[1,2-a]pyridine (6)^[34]

To a solution of 2-bromo-4'-methoxyacetophenone (**4**; 15.00 g, 65.48 mmol) in EtOH (150 mL) was added 2-amino-5-chloropyridine (**3**; 8.42 g, 65.48 mmol), and the reaction was stirred at reflux

for 2 h. NaHCO₃ (3.25 g, 38.69 mmol) was added and heating continued for another 8 h. Additional NaHCO₃ (2.25 g, 26.81 mmol) was added and stirring continued for a further 30 min. After cooling at 4 °C for 18 h, the resulting solid was collected by filtration, and washed with cold EtOH (50 mL), H₂O (100 mL), and EtOH (50 mL). The solid was then boiled with EtOH (100 mL) for 15 min, cooled, filtered, and washed with EtOH (50 mL) again and dried *in vacuo* to afford the imidazopyridine (**6**; 12.32 g, 73%) as an off-white solid. The spectroscopic data was in agreement with that previously reported. TLC (CH₂Cl₂/MeOH 95:5): $R_f = 0.85$. ¹H NMR (400 MHz, DMSO): $\delta = 8.78$ (dd, $J = 2.0, 0.8$ Hz, 1H), 8.26 (s, 1H), 7.89 (d, $J = 8.8$ Hz, 2H), 7.59 (d, $J = 9.6$ Hz, 1H), 7.26 (dd, $J = 9.6, 2.0$ Hz), 7.01 (d, $J = 8.8$ Hz, 2H), 3.81 (s, 3H). ¹³C NMR (400 MHz, DMSO): $\delta = 159.2, 145.5, 143.2, 127.0, 126.0, 125.4, 124.6, 118.7, 117.1, 114.2, 108.7, 55.1$. MS (ESI+ve) m/z 259 (³⁵Cl [M+H]⁺, 100%), 261 (³⁷Cl [M+H]⁺, 33%).

1-(6-Chloro-2-(4-methoxyphenyl)imidazo[1,2-a]pyridin-3-yl)-N,N-dimethylmethanamine (7)^[34]

To a solution of imidazopyridine (**6**; 12.00 g, 46.35 mmol) in acetic acid (145 mL) was slowly added an aqueous solution of dimethylamine (40% w/w – 74 mL, 0.58 mol), followed by aqueous formaldehyde (37% w/w – 30 mL, 0.40 mol). The resulting mixture was stirred at 55 °C for 18 h. After cooling to RT, the solution was concentrated, and the syrupy residue was dissolved in a mixture of H₂O (60 mL) and CHCl₃ (120 mL). Aqueous NaOH (10% w/v) was added dropwise until the pH was 12. The organic layer was separated, and the aqueous layer was further extracted with CHCl₃ (2×30 mL). The combined organic layers were extracted with 2 N HCl (3×60 mL) and the extract partially neutralized with NaOH (8.70 g) to pH 3. After standing at RT for 18 h, the precipitated hydroxymethyl by-product (1.03 g) was filtered. The cold filtrate (ice bath) was basified to pH 12 with NaOH, and the resulting solid was filtered, dried *in vacuo* and recrystallized from EtOH/H₂O to afford the tertiary amine (**7**; 10.05 g, 69%) as a pale-yellow crystals. The spectroscopic data was in agreement with that previously reported. TLC (CH₂Cl₂/MeOH 95:5): $R_f = 0.75$. ¹H NMR (400 MHz, DMSO): $\delta = 8.64$ (dd, $J = 2.0, 0.8$ Hz, 1H), 7.78 (d, $J = 8.8$ Hz, 2H), 7.62 (dd, $J = 9.6, 0.8$ Hz, 1H), 7.31 (dd, $J = 9.6, 2.0$ Hz, 1H), 7.04 (d, $J = 8.8$ Hz, 2H), 3.89 (s, 2H), 3.80 (s, 3H), 2.16 (s, 6H). ¹³C NMR (400 MHz, DMSO): $\delta = 159.0, 144.5, 142.3, 129.6, 126.5, 125.2, 123.5, 118.5, 117.8, 117.2, 113.9, 55.1, 51.4, 44.4$. MS (ESI+ve) m/z 316 (³⁵Cl [M+H]⁺, 100%), 318 (³⁷Cl [M+H]⁺, 33%).

1-(6-Chloro-2-(4-methoxyphenyl)imidazo[1,2-a]pyridin-3-yl)-N,N,N-trimethylmethanaminium iodide (8)^[34]

To a solution of the tertiary amine (**7**; 8.76 g, 27.83 mmol) in toluene (110 mL) was added methyl iodide (6.0 mL, 96.38 mmol), and the mixture was stirred at RT for 48 h in the dark. The precipitated solid was filtered, washed with toluene (10 mL), and dried *in vacuo* to afford the ammonium iodide (**8**; 10.66 g, 84%) as a light-yellow solid. The product was used in the next reaction step immediately or stored in the freezer for a limited time due to stability issues. The spectroscopic data was in agreement with that previously reported. TLC (CH₂Cl₂/MeOH 90:10): $R_f = 0.66$. ¹H NMR (400 MHz, DMSO): $\delta = 9.26$ (br s, 1H), 7.79 (d, $J = 8.8$ Hz, 2H), 7.75 (d, $J = 9.6$ Hz, 1H), 7.50 (dd, $J = 9.6, 2.0$ Hz, 1H), 7.06 (d, $J = 8.8$ Hz, 2H), 5.22 (s, 2H), 3.83 (s, 3H), 2.89 (s, 9H). ¹³C NMR (400 MHz, DMSO): $\delta = 159.5, 149.0, 144.2, 130.0, 127.3, 125.8, 123.3, 120.4, 118.0, 114.3, 109.8, 56.4, 55.2, 51.4$. MS (ESI+ve) m/z 330 (³⁵Cl [M], 100%), 332 (³⁷Cl [M], 33%).

2-(6-Chloro-2-(4-methoxyphenyl)imidazo[1,2-a]pyridin-3-yl)acetamide (9)^[34]

A solution of the ammonium iodide (**8**; 4.00 g, 8.74 mmol), KCN (3.90 g, 59.89 mmol), and EtOH/H₂O (1:1, 150 mL) was stirred at reflux for 48 h. The solution was cooled to RT and evaporated to dryness under a stream of N₂. H₂O (10 mL) was added and the solid was filtered, washed with H₂O (5 mL), and dried *in vacuo* to afford the acetamide (**9**; 1.96 g, 71%) as a brown solid. The spectroscopic data was in agreement with that previously reported. TLC (CH₂Cl₂/MeOH 95:5): *R*_f=0.71. ¹H NMR (400 MHz, DMSO): δ=8.61 (d, *J*=2.0 Hz, 1H), 7.80 (br s, 1H), 7.73 (d, *J*=8.8 Hz, 2H), 7.61 (d, *J*=9.6 Hz, 1H), 7.29 (dd, *J*=9.6, 2.0 Hz, 1H), 7.24 (br s, 1H), 7.05 (d, *J*=8.8 Hz, 2H), 3.98 (s, 2H), 3.81 (s, 3H). ¹³C NMR (400 MHz, DMSO): δ=170.3, 159.0, 143.5, 142.2, 129.1, 126.5, 124.8, 122.9, 118.6, 117.2, 116.1, 114.1, 55.2, 30.5. MS (ESI+ve) *m/z* 316 (³⁵Cl [M+H]⁺, 100%), 318 (³⁷Cl [M+H]⁺, 33%).

2-(6-Chloro-2-(4-methoxyphenyl)imidazo[1,2-a]pyridin-3-yl)acetic acid (10)^[39]

To a solution of acetamide (**9**; 1.60 g, 5.07 mmol) in EtOH (35 mL) was added a solution of KOH (2.42 g, 43.10 mmol) in H₂O (6.0 mL). The reaction was stirred at reflux for 18 h. The EtOH was removed and the minimum volume of H₂O was added to the residue to dissolve completely any solid material. Acidification to pH 4 with an aqueous HCl solution (12% v/v, 9 mL) precipitated the product which was filtered, washed with H₂O (20 mL), and dried *in vacuo* to afford the acid (**10**; 1.51 g, 94%) as a grey solid. TLC (CH₂Cl₂/MeOH 95:5): *R*_f=0.62. ¹H NMR (400 MHz, DMSO): δ=9.24 (br s, 1H), 7.99–7.93 (m, 2H), 7.67 (d, *J*=8.8 Hz, 2H), 7.20 (d, *J*=8.8 Hz, 2H), 4.26 (s, 2H), 3.85 (s, 3H). ¹³C NMR (400 MHz, DMSO): δ=169.8, 160.7, 138.3, 135.2, 132.5, 129.8, 125.2, 123.2, 119.2, 116.8, 114.9, 113.4, 55.5, 29.4. MS (ESI+ve) *m/z* 317 (³⁵Cl [M+H]⁺, 100%), 319 (³⁷Cl [M+H]⁺, 33%).

General Procedure A: Amide coupling

The acid (**10**; 1.0 equiv.), the appropriate mono-Boc-protected polymethylenediamine (**11a–d**; 1.2 equiv.), HOBt (1.0 equiv.), EDCI (1.3 equiv.), and DIPEA (4.0 equiv.) were combined in anhydrous DMF (6.0 mL/mmol acid), and stirred at RT for 24 h under N₂. The resulting reaction mixture was poured into H₂O (25 mL) and extracted with EtOAc (3×25 mL). The organic layer was washed with H₂O (2×25 mL), brine (2×25 mL), dried (Na₂SO₄), filtered, and concentrated. The residue was subjected to flash chromatography over SiO₂ gel (CH₂Cl₂/MeOH 95:5) to afford the desired amides **12a–d**.

***Tert*-butyl (2-(2-(6-chloro-2-(4-methoxyphenyl)imidazo[1,2-a]pyridin-3-yl)acetamido)ethyl)carbamate (12a)**

Following **General Procedure A**, acid (**10**; 220 mg, 0.69 mmol), *tert*-butyl (2-aminoethyl)carbamate (**11a**; 133 mg, 0.83 mmol), HOBt (103 mg, 0.69 mmol), EDCI (173 mg, 0.90 mmol), and DIPEA (357 mg, 2.76 mmol) were stirred in anhydrous DMF (4.1 mL) for 24 h to afford the amide (**12a**; 233 mg, 74%) as a pale-yellow oil after flash chromatography. TLC (CH₂Cl₂/MeOH 95:5): *R*_f=0.78. ¹H NMR (400 MHz, CDCl₃): δ=8.12 (br s, 1H), 7.64 (d, *J*=8.8 Hz, 2H), 7.53 (d, *J*=9.6 Hz, 1H), 7.16 (dd, *J*=9.6, 2.0 Hz, 1H), 6.99 (d, *J*=8.8 Hz, 2H), 6.71 (br s, 1H), 4.83 (br s, 1H), 3.93 (s, 2H), 3.85 (s, 3H), 3.39–3.35 (m, 2H), 3.22–3.18 (m, 2H), 1.36 (s, 9H). ¹³C NMR (400 MHz, CDCl₃): δ=168.7, 159.9, 157.2, 145.8, 143.7, 129.7, 126.2, 126.1, 121.6, 120.9, 117.8, 114.5, 113.7, 80.1, 55.5, 41.5, 40.5, 32.7, 28.4. IR (neat)_{max} 3310 (m), 3256 (m), 2935 (w), 2361 (w), 2339 (w),

1810 (w), 1770 (w), 1683 (s), 1638 (s), 1539 (s), 1465 (s), 1390 (m), 1285 (m), 1249 (s), 1174 (s), 1010 (s), 992 (s), 623 (s), 522 (s) cm⁻¹. MS (ESI+ve) *m/z* 459 (³⁵Cl [M+H]⁺, 100%), 461 (³⁷Cl [M+H]⁺, 33%). HRMS (ESI+ve TOF) calcd for C₂₃H₂₈³⁵ClN₄O₄ 459.1794, found 459.1792 ([M+H]⁺).

***Tert*-butyl (3-(2-(6-chloro-2-(4-methoxyphenyl)imidazo[1,2-a]pyridin-3-yl)acetamido)propyl)carbamate (12b)**

Following **General Procedure A**, acid (**10**; 300 mg, 0.95 mmol), *tert*-butyl (3-aminopropyl)carbamate (**11b**; 196 mg, 1.14 mmol), HOBt (141 mg, 0.95 mmol), EDCI (238 mg, 1.24 mmol), and DIPEA (491 mg, 3.80 mmol) were stirred in anhydrous DMF (5.6 mL) for 24 h to afford the amide (**12b**; 364 mg, 81%) as a pale-yellow oil after flash chromatography. TLC (CH₂Cl₂/MeOH 95:5): *R*_f=0.76. ¹H NMR (400 MHz, CDCl₃): δ=8.16 (br s, 1H), 7.68 (d, *J*=8.8 Hz, 2H), 7.55 (d, *J*=9.6 Hz, 1H), 7.16 (dd, *J*=9.6, 2.0 Hz, 1H), 6.99 (d, *J*=8.8 Hz, 2H), 6.92 (br s, 1H), 4.71 (t, *J*=5.2 Hz, 1H), 3.95 (s, 2H), 3.85 (s, 3H), 3.30–3.26 (m, 2H), 3.06–3.07 (m, 2H), 1.58–1.51 (m, 2H), 1.34 (s, 9H). ¹³C NMR (400 MHz, CDCl₃): δ=168.4, 159.8, 156.9, 145.7, 143.7, 129.7, 126.4, 125.9, 121.6, 120.8, 117.9, 114.4, 114.0, 79.7, 55.5, 36.8, 35.9, 32.8, 30.3, 28.4. IR (neat)_{max} 3344 (w), 3308 (w), 2980 (w), 2361 (w), 2340 (w), 1800 (w), 1776 (w), 1682 (s), 1644 (s), 1528 (s), 1457 (s), 1389 (m), 1364 (m), 1285 (m), 1246 (s), 1171 (s), 1027 (m), 787 (s), 626 (m), 531 (m) cm⁻¹. MS (ESI+ve) *m/z* 473 (³⁵Cl [M+H]⁺, 100%), 475 (³⁷Cl [M+H]⁺, 33%). HRMS (ESI+ve TOF) calcd for C₂₄H₃₀³⁵ClN₄O₄ 473.1950, found 473.1947 ([M+H]⁺).

***Tert*-butyl (4-(2-(6-chloro-2-(4-methoxyphenyl)imidazo[1,2-a]pyridin-3-yl)acetamido)butyl)carbamate (12c)**

Following **General Procedure A**, acid (**10**; 300 mg, 0.95 mmol), *tert*-butyl (4-aminobutyl)carbamate (**11c**; 215 mg, 1.14 mmol), HOBt (141 mg, 0.95 mmol), EDCI (238 mg, 1.24 mmol), and DIPEA (491 mg, 3.80 mmol) were stirred in anhydrous DMF (5.6 mL) for 24 h to afford the amide (**12c**; 420 mg, 91%) as a pale-yellow oil after flash chromatography. TLC (CH₂Cl₂/MeOH 95:5): *R*_f=0.71. ¹H NMR (400 MHz, DMSO): δ=8.61 (br s, 1H), 8.32 (t, *J*=5.6 Hz, 1H), 7.72 (d, *J*=8.8 Hz, 2H), 7.61 (d, *J*=9.6 Hz, 1H), 7.29 (dd, *J*=9.6, 2.0 Hz, 1H), 7.03 (d, *J*=8.8 Hz, 2H), 6.78 (t, *J*=5.6 Hz, 1H), 3.98 (s, 2H), 3.81 (s, 3H), 3.13–3.08 (m, 2H), 2.96–2.88 (m, 2H), 1.45–1.37 (m, 4H), 1.36 (s, 9H). ¹³C NMR (400 MHz, DMSO): δ=168.0, 159.0, 155.6, 143.6, 142.2, 129.1, 126.5, 124.8, 122.9, 118.6, 117.2, 115.9, 114.0, 77.3, 55.1, 40.2, 38.6, 30.7, 28.2, 27.0, 26.4. IR (neat)_{max} 3310 (w), 3256 (w), 2935 (w), 1790 (w), 1780 (w), 1682 (m), 1639 (m), 1560 (m), 1535 (m), 1500 (m), 1365 (m), 1285 (m), 1249 (s), 1174 (m), 1025 (s), 990 (s), 623 (s), 522 (s) cm⁻¹. MS (ESI+ve) *m/z* 487 (³⁵Cl [M+H]⁺, 100%), 489 (³⁷Cl [M+H]⁺, 33%). HRMS (ESI+ve TOF) calcd for C₂₅H₃₂³⁵ClN₄O₄ 487.2107, found 487.2105 ([M+H]⁺).

***Tert*-butyl (6-(2-(6-chloro-2-(4-methoxyphenyl)imidazo[1,2-a]pyridin-3-yl)acetamido)hexyl)carbamate (12d)**

Following **General Procedure A**, acid (**10**; 300 mg, 0.95 mmol), *tert*-butyl (6-aminoethyl)carbamate (**11d**; 247 mg, 1.14 mmol), HOBt (141 mg, 0.95 mmol), EDCI (238 mg, 1.24 mmol), and DIPEA (491 mg, 3.80 mmol) were stirred in anhydrous DMF (5.6 mL) for 24 h to afford the amide (**12d**; 470 mg, 96%) as a pale-yellow oil after flash chromatography. TLC (CH₂Cl₂/MeOH 95:5): *R*_f=0.70. ¹H NMR (400 MHz, DMSO): δ=8.60 (br s, 1H), 8.32 (t, *J*=5.6 Hz, 1H), 7.74 (d, *J*=8.8 Hz, 2H), 7.62 (d, *J*=9.6 Hz, 1H), 7.31 (dd, *J*=9.6, 2.0 Hz, 1H), 7.04 (d, *J*=8.8 Hz, 2H), 6.74 (t, *J*=5.6 Hz, 1H), 3.98 (s, 2H), 3.81 (s, 3H), 3.13–3.08 (m, 2H), 2.91–2.87 (m, 2H), 1.46–1.21 (m, 8H), 1.36 (s, 9H). ¹³C NMR (400 MHz, DMSO): δ=168.1, 159.1, 155.7, 143.6, 142.3, 129.3, 126.5, 125.0, 122.9, 118.8, 117.3, 116.0,

114.1, 77.5, 55.2, 40.0, 39.0, 30.8, 29.6, 29.1, 28.4, 26.2, 26.1. IR (neat)_{max} 3292 (w), 2931 (w), 1800 (w), 1776 (w), 1688 (s), 1651 (s), 1500 (s), 1456 (m), 1390 (s), 1364 (s), 1329 (m), 1248 (s), 1172 (s), 1026 (s), 837 (s), 799 (s), 626 (s) cm⁻¹. MS (ESI+ve) *m/z* 515 (³⁵Cl [M+H]⁺, 100%), 517 (³⁷Cl [M+H]⁺, 33%). HRMS (ESI+ve TOF) calcd for C₂₇H₃₆³⁵ClN₄O₄ 515.2420, found 515.2429 ([M+H]⁺).

General Procedure B: Amine deprotection

The N-protected amine (**12a–d**; 1.0 equiv.) in CH₂Cl₂ (10 mL/mmol amine) was treated with CF₃CO₂H (3 mL/mmol amine). The reaction mixture was stirred at RT for 4 h followed by removal of the solvent. The residue was dissolved in EtOAc (25 mL), neutralized with saturated aqueous NaHCO₃, and then washed with H₂O (2×25 mL). The organic layer was dried (Na₂SO₄) and concentrated. The residue was subjected to flash chromatography over SiO₂ gel (CH₂Cl₂/MeOH 95:5) to afford the desired free amines **13a–d**.

N-(2-Aminoethyl)-2-(6-chloro-2-(4-methoxyphenyl)imidazo[1,2-a]pyridin-3-yl)acetamide (**13a**)

Following **General Procedure B**, N-protected amine (**12a**; 110 mg, 0.24 mmol) was dissolved in CHCl₃ (2.4 mL) and treated with CF₃CO₂H (0.7 mL) to afford the free amine (**13a**; 75 mg, 87%) as a pale-yellow foam that collapsed into a translucent gum after flash chromatography. TLC (CH₂Cl₂/MeOH 95:5): *R*_f=0.50. ¹H NMR (400 MHz, DMSO): δ=8.59 (br s, 1H), 8.49 (t, *J*=5.6 Hz, 1H), 7.68 (d, *J*=8.8 Hz, 2H), 7.61 (d, *J*=9.2 Hz, 1H), 7.31 (dd, *J*=9.2, 2.0 Hz, 1H), 7.04 (d, *J*=8.8 Hz, 2H), 4.03 (s, 2H), 3.80 (s, 3H), 3.47 (br s, 2H), 3.38 (t, *J*=6.0 Hz, 2H), 2.92 (t, *J*=6.0 Hz, 2H). ¹³C NMR (400 MHz, DMSO): δ=169.3, 159.1, 143.8, 142.4, 129.3, 126.5, 125.2, 123.1, 118.8, 117.3, 115.6, 114.2, 55.3, 38.9, 36.9, 30.8. IR (neat)_{max} 3336 (w), 3085 (w), 2944 (w), 1779 (m), 1661 (m), 1563 (m), 1509 (m), 1260 (m), 1224 (s), 1140 (s), 1026 (m), 834 (s), 809 (s), 704 (s), 517 (s) cm⁻¹. MS (ESI+ve) *m/z* 359 (³⁵Cl [M+H]⁺, 100%), 361 (³⁷Cl [M+H]⁺, 33%). HRMS (ESI+ve TOF) calcd for C₁₈H₂₀³⁵ClN₄O₂ 359.1269, found 359.1263 ([M+H]⁺).

N-(3-Aminopropyl)-2-(6-chloro-2-(4-methoxyphenyl)imidazo[1,2-a]pyridin-3-yl)acetamide (**13b**)

Following **General Procedure B**, N-protected amine (**12b**; 200 mg, 0.42 mmol) was dissolved in CHCl₃ (4.2 mL) and treated with CF₃CO₂H (1.3 mL) to afford the free amine (**13b**; 140 mg, 89%) as a pale-yellow foam that collapsed into a translucent gum after flash chromatography. TLC (CH₂Cl₂/MeOH 95:5): *R*_f=0.49. ¹H NMR (400 MHz, DMSO): δ=8.89 (br s, 1H), 8.54 (t, *J*=5.6 Hz, 1H), 7.89–7.79 (m, 3H), 7.70 (d, *J*=8.8 Hz, 2H), 7.64 (d, *J*=9.2 Hz, 1H), 7.12 (d, *J*=8.8 Hz, 2H), 4.07 (s, 2H), 3.83 (s, 3H), 3.26–3.23 (m, 2H), 2.86–2.76 (m, 2H), 1.76 (quint, *J*=6.0 Hz, 2H). ¹³C NMR (400 MHz, DMSO): δ=167.7, 161.2, 138.6, 135.1, 133.1, 130.4, 125.8, 123.8, 119.5, 118.2, 115.4, 113.6, 56.0, 37.1, 36.6, 30.4, 27.5. IR (neat)_{max} 3370 (w), 2962 (w), 2728 (w), 1656 (s), 1508 (m), 1420 (m), 1354 (m), 1301 (m), 1255 (m), 1174 (s), 1125 (s), 1019 (m), 833 (s), 795 (s), 720 (s), 518 (s) cm⁻¹. MS (ESI+ve) *m/z* 373 (³⁵Cl [M+H]⁺, 100%), 375 (³⁷Cl [M+H]⁺, 33%). HRMS (ESI+ve TOF) calcd for C₁₉H₂₂³⁵ClN₄O₂ 373.1426, found 373.1424 ([M+H]⁺).

N-(4-Aminobutyl)-2-(6-chloro-2-(4-methoxyphenyl)imidazo[1,2-a]pyridin-3-yl)acetamide (**13c**)

Following **General Procedure B**, N-protected amine (**12c**; 200 mg, 0.41 mmol) was dissolved in CHCl₃ (4.1 mL) and treated with

CF₃CO₂H (1.2 mL) to afford the free amine (**13c**; 85%) as a pale-yellow foam that collapsed into a translucent gum after flash chromatography. TLC (CH₂Cl₂/MeOH 95:5): *R*_f=0.46. ¹H NMR (400 MHz, DMSO): δ=8.87 (br s, 1H), 8.47 (t, *J*=5.6 Hz, 1H), 7.90–7.80 (m, 3H), 7.70 (d, *J*=8.8 Hz, 2H), 7.63 (d, *J*=9.2 Hz, 1H), 7.12 (d, *J*=8.8 Hz, 2H), 4.05 (s, 2H), 3.84 (s, 3H), 3.15–3.11 (m, 2H), 2.85–2.76 (m, 2H), 1.60–1.46 (m, 4H). ¹³C NMR (400 MHz, DMSO): δ=167.5, 161.1, 138.5, 134.9, 133.1, 130.4, 125.8, 123.7, 119.5, 118.3, 115.3, 113.6, 60.0, 38.7, 38.7, 30.4, 26.4, 24.8. IR (neat)_{max} 3300 (w), 3161 (w), 2960 (w), 1777 (w), 1640 (m), 1611 (m), 1555 (m), 1510 (m), 1260 (m), 1180 (s), 1130 (s), 1023 (m), 906 (m), 820 (s), 796 (s), 704 (s), 518 (s) cm⁻¹. MS (ESI+ve) *m/z* 387 (³⁵Cl [M+H]⁺, 100%), 389 (³⁷Cl [M+H]⁺, 33%). HRMS (ESI+ve TOF) calcd for C₂₀H₂₄³⁵ClN₄O₂ 387.1582, found 387.1583 ([M+H]⁺).

N-(6-Aminoethyl)-2-(6-chloro-2-(4-methoxyphenyl)imidazo[1,2-a]pyridin-3-yl)acetamide (**13d**)

Following **General Procedure B**, N-protected amine (**12d**; 225 mg, 0.44 mmol) was dissolved in CHCl₃ (4.4 mL) and treated with CF₃CO₂H (1.3 mL) to afford the free amine (**13d**; 160 mg, 87%) as a pale-yellow foam that collapsed into a translucent gum after flash chromatography. TLC (CH₂Cl₂/MeOH 95:5): *R*_f=0.45. ¹H NMR (400 MHz, DMSO): δ=9.22 (br s, 1H), 8.68 (t, *J*=5.6 Hz, 1H), 8.05 (br s, 2H), 7.99–7.93 (m, 2H), 7.77 (d, *J*=8.8 Hz, 2H), 7.16 (d, *J*=8.8 Hz, 2H), 4.14 (s, 2H), 3.85 (s, 3H), 3.14–3.09 (m, 2H), 2.77–2.69 (m, 2H), 1.58–1.24 (m, 8H). ¹³C NMR (400 MHz, DMSO): δ=167.3, 161.1, 138.8, 135.6, 132.6, 130.4, 125.6, 123.5, 120.0, 118.3, 115.2, 113.9, 56.0, 30.4, 29.2, 27.3, 27.2, 26.4, 26.0, 25.8. IR (neat)_{max} 3337 (w), 3086 (w), 2943 (w), 1779 (m), 1661 (m), 1609 (m), 1563 (m), 1510 (m), 1240 (m), 1139 (s), 1026 (s), 908 (m), 834 (s), 784 (s), 704 (s), 516 (s) cm⁻¹. MS (ESI+ve) *m/z* 415 (³⁵Cl [M+H]⁺, 100%), 417 (³⁷Cl [M+H]⁺, 33%). HRMS (ESI+ve TOF) calcd for C₂₂H₂₈³⁵ClN₄O₂ 415.1895, found 415.1895 ([M+H]⁺).

General Procedure C: Synthesis of fluorescent probes

The amine (**13a–d**; 1.0 equiv.) was dissolved in anhydrous DMF (20 mL/mmol amine) with magnetic stirring. The solution was brought to 0 °C (ice bath) followed by sequential dropwise addition of DIPEA (1.4 equiv.) and a solution of NBD-Cl (**14**; 1.0 equiv.) in DMF (1.0 mL) under a flow of N₂ gas. The reaction vessel was then sealed and allowed to warm to RT and stirring was continued for 18 h under N₂ in the dark. The solution was partitioned between CHCl₃ (100 mL) and H₂O (100 mL). The aqueous phase was separated and extracted with CHCl₃ (5×50 mL). The combined organic extracts were washed with H₂O (2×100 mL), brine (2×100 mL), dried (Na₂SO₄), filtered, and concentrated. The residue was purified by preparative TLC plate chromatography to afford the desired fluorescent probes **15a–d**.

2-(6-Chloro-2-(4-methoxyphenyl)imidazo[1,2-a]pyridin-3-yl)-N-(2-((7-nitrobenzo[c][1,2,5]oxadiazol-4-yl)amino)ethyl)acetamide (**15a**)

Following **General Procedure C**, amine (**13a**; 40 mg, 0.11 mmol) was dissolved in DMF (1.1 mL) followed by sequential addition of DIPEA (19 mg, 0.15 mmol) and NBD-Cl (**14**; 22 mg, 0.11 mmol) to afford the desired fluorescent probe (**15a**; 31 mg, 54%) as a light-brown solid after preparative TLC plate chromatography (CH₂Cl₂/MeOH 95:5). TLC (CH₂Cl₂/MeOH 95:5): *R*_f=0.33. mp 206–208 °C. ¹H NMR (500 MHz, DMSO): δ=9.31 (br s, 1H), 8.54–8.48 (m, 2H), 8.31 (d, *J*=8.5 Hz, 1H), 7.71 (d, *J*=8.5 Hz, 2H), 7.57 (d, *J*=9.5 Hz, 1H), 7.20 (d, *J*=9.5 Hz, 1H), 6.92 (d, *J*=8.5 Hz, 2H), 6.31 (d, *J*=8.5 Hz, 1H), 3.97 (s, 2H), 3.77 (s, 3H), 3.60 (br s, 2H), 3.50–3.45 (m,

2H). ^{13}C NMR (500 MHz, DMSO): $\delta = 169.4, 159.4, 145.9, 144.8, 144.5, 144.1, 142.7, 138.2, 129.5, 126.8, 125.3, 123.1, 121.4, 119.1, 117.6, 115.7, 114.3, 99.3, 55.5, 43.2, 38.4, 31.3$. IR (neat) $_{\text{max}}$ 3363 (w), 3276 (w), 3100 (w), 1760 (w), 1654 (m), 1632 (m), 1589 (s), 1539 (s), 1517 (s), 1303 (s), 1137 (s), 1022 (m), 999 (s), 828 (s), 778 (s), 738 (s), 623 (s) cm^{-1} . MS (ESI $-$ ve) m/z 520 (^{35}Cl [M $-$ H] $^{-}$, 100%), 522 (^{37}Cl [M $-$ H] $^{-}$, 33%). HRMS (ESI $-$ ve TOF) calcd for $\text{C}_{24}\text{H}_{19}^{35}\text{ClN}_7\text{O}_5$ 520.1142, found 520.1136 ([M $-$ H] $^{-}$).

2-(6-Chloro-2-(4-methoxyphenyl)imidazo[1,2-a]pyridin-3-yl)-N-(3-((7-nitrobenzo[c][1,2,5]oxadiazol-4-yl)amino)propyl)acetamide (15 b)

Following **General Procedure C**, amine (**13 b**; 150 mg, 0.40 mmol) was dissolved in DMF (3.0 mL) followed by sequential addition of DIPEA (72 mg, 0.56 mmol) and NBD-Cl (**14**; 80 mg, 0.40 mmol) to afford the desired fluorescent probe (**15 b**; 90 mg, 42%) as a light-brown solid after preparative TLC plate chromatography ($\text{CH}_2\text{Cl}_2/\text{MeOH}$ 90:10). TLC ($\text{CH}_2\text{Cl}_2/\text{MeOH}$ 90:10): $R_f = 0.48$. mp 207–209 °C. ^1H NMR (400 MHz, DMSO): $\delta = 9.47$ (t, $J = 4.4$ Hz, 1H), 8.64 (br s, 1H), 8.47 (d, $J = 9.2$ Hz, 1H), 8.38 (t, $J = 4.4$ Hz, 1H), 7.73 (d, $J = 8.8$ Hz, 2H), 7.62 (d, $J = 9.6$ Hz, 1H), 7.29 (dd, $J = 9.6, 2.0$ Hz, 1H), 7.01 (d, $J = 8.8$ Hz, 2H), 6.34 (d, $J = 9.2$ Hz, 1H), 4.02 (s, 2H), 3.78 (s, 3H), 3.49 (br s, 2H), 3.28–3.23 (m, 2H), 1.92–1.85 (m, 2H). ^{13}C NMR (400 MHz, DMSO): $\delta = 168.8, 159.5, 145.6, 144.9, 144.6, 143.9, 142.6, 138.3, 129.6, 126.8, 125.5, 123.4, 121.3, 119.2, 117.6, 116.2, 114.5, 99.5, 55.6, 41.6, 37.0, 31.2, 28.1$. IR (neat) $_{\text{max}}$ 3231 (w), 3072 (w), 2966 (w), 1717 (w), 1633 (m), 1582 (m), 1523 (m), 1495 (m), 1446 (m), 1293 (s), 1249 (s), 1175 (s), 1137 (s), 1010 (m), 802 (s), 597 (s), 526 (s) cm^{-1} . MS (ESI $-$ ve) m/z 534 (^{35}Cl [M $-$ H] $^{-}$, 100%), 536 (^{37}Cl [M $-$ H] $^{-}$, 33%). HRMS (ESI $-$ ve TOF) calcd for $\text{C}_{25}\text{H}_{21}^{35}\text{ClN}_7\text{O}_5$ 534.1298, found 534.1305 ([M $-$ H] $^{-}$).

2-(6-Chloro-2-(4-methoxyphenyl)imidazo[1,2-a]pyridin-3-yl)-N-(4-((7-nitrobenzo[c][1,2,5]oxadiazol-4-yl)amino)butyl)acetamide (15 c)

Following **General Procedure C**, amine (**13 c**; 100 mg, 0.26 mmol) was dissolved in DMF (1.6 mL) followed by sequential addition of DIPEA (47 mg, 0.36 mmol) and NBD-Cl (**14**; 52 mg, 0.26 mmol) to afford the desired fluorescent probe (**15 c**; 82 mg, 57%) as a light-brown solid after preparative TLC plate chromatography ($\text{CH}_2\text{Cl}_2/\text{MeOH}$ 93:7). TLC ($\text{CH}_2\text{Cl}_2/\text{MeOH}$ 93:7): $R_f = 0.31$. mp 208–209 °C. ^1H NMR (500 MHz, DMSO): $\delta = 9.55$ (t, $J = 4.4$ Hz, 1H), 8.61 (s, 1H), 8.40 (d, $J = 9.2$ Hz, 1H), 8.36 (t, $J = 4.4$ Hz, 1H), 7.72 (d, $J = 8.8$ Hz, 2H), 7.61 (d, $J = 9.6$ Hz, 1H), 7.27 (d, $J = 9.6$ Hz, 1H), 6.99 (d, $J = 8.8$ Hz, 2H), 6.38 (d, $J = 9.2$ Hz, 1H), 3.97 (s, 2H), 3.77 (s, 3H), 3.46 (br s, 2H), 3.22–3.16 (m, 2H), 1.74–1.66 (m, 2H), 1.61–1.53 (m, 2H). ^{13}C NMR (500 MHz, DMSO): $\delta = 168.6, 159.4, 145.6, 144.9, 142.6, 138.4, 133.0, 131.0, 129.6, 126.8, 125.4, 123.4, 121.1, 119.1, 117.6, 116.4, 114.4, 99.5, 55.6, 44.4, 38.8, 31.2, 27.0, 25.5$. IR (neat) $_{\text{max}}$ 3368 (w), 3218 (w), 3081 (w), 2914 (w), 1735 (w), 1661 (m), 1620 (m), 1564 (m), 1506 (m), 1461 (m), 1316 (s), 1231 (s), 1172 (s), 1017 (s), 908 (m), 829 (s), 807 (s), 741 (s), 599 (s), 523 (s) cm^{-1} . MS (ESI $+$ ve) m/z 550 (^{35}Cl [M+H] $^{+}$, 100%), 552 (^{37}Cl [M+H] $^{+}$, 33%). HRMS (ESI $+$ ve TOF) calcd for $\text{C}_{26}\text{H}_{25}^{35}\text{ClN}_7\text{O}_5$ 550.1600, found 550.1601 ([M+H] $^{+}$).

2-(6-Chloro-2-(4-methoxyphenyl)imidazo[1,2-a]pyridin-3-yl)-N-(6-((7-nitrobenzo[c][1,2,5]oxadiazol-4-yl)amino)hexyl)acetamide (15 d)

Following **General Procedure C**, amine (**13 d**; 100 mg, 0.24 mmol) was dissolved in DMF (1.4 mL) followed by sequential addition of DIPEA (44 mg, 0.34 mmol) and NBD-Cl (**14**; 48 mg, 0.24 mmol) to afford the desired fluorescent probe (**15 d**; 78 mg, 56%) as a light-

brown solid after preparative TLC plate chromatography ($\text{CH}_2\text{Cl}_2/\text{MeOH}$ 90:10). TLC ($\text{CH}_2\text{Cl}_2/\text{MeOH}$ 90:10): $R_f = 0.30$. mp 210–211 °C. ^1H NMR (400 MHz, DMSO): $\delta = 9.53$ (t, $J = 4.4$ Hz, 1H), 8.60 (s, 1H), 8.48 (d, $J = 9.2$ Hz, 1H), 8.32 (t, $J = 4.4$ Hz, 1H), 7.73 (d, $J = 8.8$ Hz, 2H), 7.60 (d, $J = 9.6$ Hz, 1H), 7.27 (dd, $J = 9.6, 2.0$ Hz, 1H), 7.00 (d, $J = 8.8$ Hz, 2H), 6.36 (d, $J = 9.2$ Hz, 1H), 3.98 (s, 2H), 3.78 (s, 3H), 3.33 (br s, 2H), 3.15–3.10 (m, 2H), 1.69 (quint, $J = 6.4$ Hz, 2H), 1.48 (quint, $J = 6.4$ Hz, 2H), 1.46–1.35 (m, 4H). ^{13}C NMR (400 MHz, DMSO): $\delta = 168.0, 158.9, 145.1, 144.4, 144.1, 143.5, 142.1, 137.9, 129.1, 126.4, 124.9, 122.8, 120.5, 118.6, 117.2, 115.9, 113.9, 99.0, 55.1, 43.3, 38.7, 30.7, 28.9, 27.6, 26.1, 26.0$. IR (neat) $_{\text{max}}$ 3255 (w), 3225 (w), 2922 (w), 2852 (w), 1640 (w), 1650 (w), 1615 (m), 1527 (m), 1496 (m), 1442 (m), 1292 (s), 1245 (s), 1173 (s), 1025 (m), 998 (m), 903 (m), 836 (m), 801 (m), 739 (m), 595 (s), 520 (s) cm^{-1} . MS (ESI $+$ ve) m/z 578 (^{35}Cl [M+H] $^{+}$, 100%), 580 (^{37}Cl [M+H] $^{+}$, 33%). HRMS (ESI $+$ ve TOF) calcd for $\text{C}_{28}\text{H}_{29}^{35}\text{ClN}_7\text{O}_5$ 578.1913, found 578.1911 ([M+H] $^{+}$).

7-Nitrobenzo[c][1,2,5]oxadiazol-4-amine (16)^{40j}

To a stirred solution of 4-chloro-7-nitrobenzofurazan (**14**; 500 mg, 2.51 mmol) in MeOH (25 mL) at 0 °C (ice bath) was added dropwise NH_4OH (30% v/v – 10 mL, 1.48 mol). The reaction was allowed to warm to RT and stirring was continued for 24 h under N_2 in the dark. The solvent was evaporated *in vacuo*, and the residue was purified by flash chromatography over SiO_2 gel (EtOAc/hexanes 70:30) to afford the NBD amine (**16**; 229 mg, 51%) as a dark-brown solid. The spectroscopic data was in agreement with that previously reported. TLC (EtOAc/hexanes 70:30): $R_f = 0.50$. ^1H NMR (400 MHz, DMSO): $\delta = 8.83$ (br s, 2H), 8.45 (d, $J = 8.8$ Hz, 1H), 6.37 (d, $J = 8.8$ Hz, 1H). ^{13}C NMR (400 MHz, DMSO): $\delta = 147.7, 144.6, 144.4, 138.3, 120.8, 103.1$. MS (ESI $-$ ve) m/z 179 ([M $-$ H] $^{-}$, 100%).

2-(6-Chloro-2-(4-methoxyphenyl)imidazo[1,2-a]pyridin-3-yl)-N-(7-nitrobenzo[c][1,2,5]oxadiazol-4-yl)acetamide (17)

To a stirred solution of the acid (**10**; 33 mg, 0.10 mmol) in anhydrous DMF (2.0 mL) was added HOBt (15 mg, 0.10 mmol), EDCI (25 mg, 0.13 mmol), DIPEA (52 mg, 0.40 mmol), and the NBD- NH_2 (**16**; 20 mg, 0.10 mmol). Stirring was prolonged at RT for 48 h, and the resulting reaction mixture was poured into H_2O (25 mL) and extracted with EtOAc (3 \times 25 mL). The organic solution was separated, washed with H_2O (2 \times 25 mL), brine (2 \times 25 mL), dried (Na_2SO_4), filtered, and concentrated. The residue was subjected to flash chromatography over SiO_2 gel ($\text{CH}_2\text{Cl}_2/\text{MeOH}$ 95:5) to afford the desired fluorescent probe (**17**; 30 mg, 62%) as a light-brown solid. TLC ($\text{CH}_2\text{Cl}_2/\text{MeOH}$ 95:5): $R_f = 0.63$. mp 167–169 °C. ^1H NMR (500 MHz, CD_3OD): $\delta = 8.97$ (br s, 1H), 8.47 (d, $J = 8.0$ Hz, 1H), 7.92–7.87 (m, 1H), 7.85 (d, $J = 8.0$ Hz, 1H), 7.64 (d, $J = 9.0$ Hz, 2H), 7.16 (d, $J = 9.0$ Hz, 2H), 6.40 (d, $J = 8.0$ Hz, 1H), 4.22 (s, 2H), 3.89 (s, 3H). ^{13}C NMR (500 MHz, CD_3OD): $\delta = 171.7, 163.0, 148.5, 148.2, 145.6, 145.6, 140.3, 138.4, 138.1, 134.0, 131.2, 126.2, 125.8, 120.6, 118.3, 116.1, 114.3, 103.2, 56.1, 30.1$. IR (neat) $_{\text{max}}$ 3335 (w), 2930 (w), 1700 (w), 1647 (w), 1558 (m), 1539 (s), 1507 (m), 1251 (s), 1174 (s), 1024 (s), 992 (s), 796 (s), 732 (s), 612 (s) cm^{-1} . MS (ESI $-$ ve) m/z 477 (^{35}Cl [M $-$ H] $^{-}$, 100%), 479 (^{37}Cl [M $-$ H] $^{-}$, 33%). HRMS (ESI $-$ ve TOF) calcd for $\text{C}_{22}\text{H}_{14}^{35}\text{ClN}_6\text{O}_5$ 477.0720, found 477.0714 ([M $-$ H] $^{-}$).

2-(6-Chloro-2-(4-hydroxyphenyl)imidazo[1,2-a]pyridin-3-yl)acetic acid hydrobromide hydrate (18)^{34j}

Acetamide (**9**; 1.60 g, 5.07 mmol) was dissolved in acetic acid (12.5 mL, 0.21 mol) with magnetic stirring, and the solution was brought to 0 °C (ice bath). HBr (48% w/w – 25 mL, 0.11 mol) was added dropwise, the ice bath removed, and the reaction solution

heated to 110 °C for 48 h. The solution was cooled to RT, then placed at 4 °C for 18 h to give a brown precipitate. The precipitate was filtered, washed with acetic acid (10 mL), and dried *in vacuo* to afford the acid (**18**; 1.22 g, 63%) as a light-brown solid. The spectroscopic data was in agreement with that previously reported. TLC (CH₂Cl₂/MeOH 90:5): *R*_f=0.58. ¹H NMR (400 MHz, DMSO): δ = 10.16 (br s, 1H), 9.28 (s, 1H), 8.03–7.96 (m, 2H), 7.52 (d, *J* = 8.8 Hz, 2H), 7.02 (d, *J* = 8.8 Hz, 2H), 4.24 (s, 2H). ¹³C NMR (400 MHz, DMSO): δ = 169.8, 159.4, 137.9, 135.1, 132.8, 129.9, 125.4, 123.5, 117.1, 116.7, 116.3, 113.2, 29.3. MS (ESI+ve) *m/z* 303 (³⁵Cl [M+H]⁺, 100%), 305 (³⁷Cl [M+H]⁺, 33%).

2-(6-Chloro-2-(4-hydroxyphenyl)imidazo[1,2-a]pyridin-3-yl)-N,N-diethylacetamide (**19**)^[34]

A mixture of acid (**18**; 830 mg, 2.16 mmol), HOBT (295 mg, 2.16 mmol), EDCI (539 mg, 2.81 mmol), diethylamine (268 μL, 2.59 mmol), and DIPEA (1.58 mL, 8.64 mmol) was stirred in anhydrous DMF (8 mL) at RT for 24 h under N₂. H₂O (43 mL) and acetic acid (0.4 mL) were added, stirred for 5 min, and placed at 4 °C for 18 h to give a brown precipitate which was filtered, washed with H₂O (20 mL), and dried *in vacuo*. Anhydrous DMF (4.0 mL) and diethylamine (0.4 mL) were added to the crude product and heated to 110 °C for 6 h until the diethylamine was evaporated from the solution. After cooling to 80 °C, EtOAc (8.0 mL) was added rapidly. The solution was cooled to 4 °C for 18 h to form a white crystalline solid, which was filtered, washed with cold ethyl acetate (4.0 mL), and dried *in vacuo* to afford diethylamide (**19**; 570 mg, 74%) as white needles. The spectroscopic data was in agreement with that previously reported. TLC (CH₂Cl₂/MeOH 95:5): *R*_f=0.67. ¹H NMR (400 MHz, DMSO): δ = 9.62 (br s, 1H), 8.50 (dd, *J* = 0.8, 2.0 Hz, 1H), 7.59 (dd, *J* = 9.6, 0.8 Hz, 1H), 7.42 (d, *J* = 8.8 Hz, 2H), 7.27 (dd, *J* = 9.6, 2.0 Hz, 1H), 6.84 (d, *J* = 8.8 Hz, 2H), 4.18 (s, 2H), 3.44 (q, *J* = 7.2 Hz, 2H), 3.32 (q, *J* = 7.2 Hz, 2H), 1.16 (t, *J* = 7.2 Hz, 3H), 1.06 (t, *J* = 7.2 Hz, 3H). ¹³C NMR (400 MHz, DMSO): δ = 167.1, 157.2, 143.9, 142.1, 129.1, 125.0, 124.5, 123.0, 118.3, 117.0, 116.1, 115.4, 41.7, 39.9, 28.7, 14.1, 13.1. MS (ESI+ve) *m/z* 358 (³⁵Cl [M+H]⁺, 100%), 360 (³⁷Cl [M+H]⁺, 33%).

General Procedure D: Phenol alkylation

To a stirred solution of the phenol (**19**; 1.0 equiv.) in anhydrous DMF (15 mL/mmol phenol) was added K₂CO₃ (4.0 equiv.) and the appropriate Boc-protected bromoamine (**20 a–b**; 1.2 equiv.). Stirring was prolonged at RT for 48 h under N₂, and the resulting reaction mixture was poured into H₂O (25 mL) and extracted with EtOAc (3 × 25 mL). The organic solution was separated, washed with H₂O (2 × 25 mL), brine (2 × 25 mL), dried (Na₂SO₄), filtered, and concentrated. The residue was purified by preparative TLC plate chromatography (CH₂Cl₂/MeOH 95:5) to afford the desired *O*-alkylated phenols **21 a–b**.

Tert-butyl (2-(4-(6-chloro-3-(2-(diethylamino)-2-oxoethyl)imidazo[1,2-a]pyridin-2-yl)phenoxy)ethyl)carbamate (**21 a**)

Following **General Procedure D**, phenol (**19**; 250 mg, 0.70 mmol) was dissolved in anhydrous DMF (10.5 mL) followed by sequential addition of K₂CO₃ (387 mg, 28 mmol) and *tert*-butyl (2-bromoethyl)carbamate (**20 a**; 188 mg, 0.84 mmol) to afford the *O*-alkylated phenol (**21 a**; 250 mg, 71%) as a pale-yellow foam after preparative TLC plate chromatography. TLC (CH₂Cl₂/MeOH 95:5): *R*_f=0.74. NMR (400 MHz, DMSO): δ = 8.52 (br s, 1H), 7.60 (d, *J* = 9.6 Hz, 1H), 7.52 (d, *J* = 8.8 Hz, 2H), 7.28 (dd, *J* = 9.6, 2.0 Hz, 1H), 7.05–7.01 (m, 3H), 4.20 (s, 2H), 4.01 (t, *J* = 6.4 Hz, 2H), 3.45 (q, *J* = 7.2 Hz, 2H),

3.36–3.29 (m, 4H), 1.39 (s, 9H), 1.16 (t, *J* = 7.2 Hz, 3H), 1.07 (t, *J* = 7.2 Hz, 3H). ¹³C NMR (400 MHz, DMSO): δ = 167.0, 158.2, 155.7, 143.4, 142.2, 129.0, 126.7, 124.7, 123.0, 118.4, 117.1, 116.4, 114.6, 77.8, 66.5, 63.6, 41.7, 38.3, 28.7, 28.2, 14.1, 13.0. IR (neat)_{max} 3458 (w), 3273 (w), 2975 (w), 1703 (m), 1638 (m), 1500 (m), 1390 (w), 1245 (m), 1171 (m), 1035 (s), 1025 (s), 1010 (s), 820 (m), 758 (m), 525 (m) cm⁻¹. MS (ESI+ve) *m/z* 501 (³⁵Cl [M+H]⁺, 100%), 503 (³⁷Cl [M+H]⁺, 33%). HRMS (ESI+ve TOF) calcd for C₂₆H₃₄³⁵ClN₄O₄ 501.2263, found 501.2269 ([M+H]⁺).

Tert-butyl (3-(4-(6-chloro-3-(2-(diethylamino)-2-oxoethyl)imidazo[1,2-a]pyridin-2-yl)phenoxy)propyl)carbamate (**21 b**)

Following **General Procedure D**, phenol (**19**; 250 mg, 0.70 mmol) was dissolved in anhydrous DMF (10.5 mL) followed by sequential addition of K₂CO₃ (387 mg, 28 mmol) and *tert*-butyl (3-bromopropyl)carbamate (**20 b**; 200 mg, 0.84 mmol) to afford the *O*-alkylated phenol (**21 b**; 261 mg, 72%) as a pale-yellow foam after preparative TLC plate chromatography. TLC (CH₂Cl₂/MeOH 95:5): *R*_f=0.76. NMR (400 MHz, DMSO): δ = 8.51 (br s, 1H), 7.60 (d, *J* = 9.6 Hz, 1H), 7.52 (d, *J* = 8.8 Hz, 2H), 7.27 (dd, *J* = 9.6, 2.0 Hz, 1H), 7.01 (d, *J* = 8.8 Hz, 2H), 6.90 (t, *J* = 5.2 Hz, 1H), 4.20 (s, 2H), 4.02 (t, *J* = 6.4 Hz, 2H), 3.44 (q, *J* = 7.2 Hz, 2H), 3.33 (q, *J* = 7.2 Hz, 2H), 3.12–3.08 (m, 2H), 1.85 (quint, *J* = 6.4 Hz, 2H), 1.38 (s, 9H), 1.17 (t, *J* = 7.2 Hz, 3H), 1.07 (t, *J* = 7.2 Hz, 3H). ¹³C NMR (400 MHz, DMSO): δ = 167.0, 158.3, 155.6, 143.4, 142.2, 129.0, 126.5, 124.7, 123.0, 118.4, 117.1, 116.4, 114.5, 77.5, 65.3, 63.6, 41.7, 36.9, 29.2, 28.7, 28.2, 14.1, 13.0. IR (neat)_{max} 3394 (w), 3250 (w), 2974 (w), 1633 (m), 1501 (m), 1391 (w), 1332 (w), 1248 (m), 1048 (m), 1037 (s), 998 (s), 823 (m), 761 (m), 525 (m) cm⁻¹. MS (ESI+ve) *m/z* 515 (³⁵Cl [M+H]⁺, 100%), 517 (³⁷Cl [M+H]⁺, 33%). HRMS (ESI+ve TOF) calcd for C₂₇H₃₆³⁵ClN₄O₄ 515.2420, found 515.2426 ([M+H]⁺).

General Procedure E: Amine deprotection

The *O*-alkylated phenol (**21 a–b**; 1.0 equiv.) in CH₂Cl₂ (10 mL/mmol amine) was treated with CF₃CO₂H (3 mL/mmol amine). The reaction mixture was stirred at RT for 4 h followed by removal of the solvent. The residue was dissolved in EtOAc (25 mL), neutralized with saturated aqueous NaHCO₃, and then washed with H₂O (2 × 25 mL). The organic layer was dried (Na₂SO₄) and concentrated. The residue was purified by preparative TLC plate chromatography (CH₂Cl₂/MeOH 95:5) to afford the desired free amines **22 a–b**.

2-(2-(4-(2-Aminoethoxy)phenyl)-6-chloroimidazo[1,2-a]pyridin-3-yl)-N,N-diethylacetamide (**22 a**)

Following **General Procedure E**, *O*-alkylated phenol (**21 a**; 200 mg, 0.40 mmol) was dissolved in CHCl₃ (4.0 mL) and treated with CF₃CO₂H (1.2 mL) to afford the free amine (**22 a**; 141 mg, 88%) a pale-yellow foam that collapsed into a translucent gum after preparative TLC plate chromatography. TLC (CH₂Cl₂/MeOH 95:5): *R*_f=0.50. NMR (400 MHz, DMSO): δ = 8.53 (br s, 1H), 7.61 (d, *J* = 9.6 Hz, 1H), 7.54 (d, *J* = 8.8 Hz, 2H), 7.29 (dd, *J* = 9.6, 2.0 Hz, 1H), 7.05 (d, *J* = 8.8 Hz, 2H), 4.22 (s, 2H), 4.00 (t, *J* = 5.6 Hz, 2H), 3.46 (q, *J* = 7.2 Hz, 2H), 3.38–3.24 (m, 4H), 2.94 (t, *J* = 5.6 Hz, 2H), 1.18 (t, *J* = 7.2 Hz, 3H), 1.08 (t, *J* = 7.2 Hz, 3H). ¹³C NMR (400 MHz, DMSO): δ = 167.0, 158.3, 143.4, 142.2, 129.0, 126.6, 124.7, 123.0, 118.4, 117.1, 116.4, 114.6, 69.6, 41.7, 40.6, 40.2, 28.7, 14.2, 13.1. IR (neat)_{max} 3303 (w), 2973 (w), 2932 (w), 1699 (m), 1634 (m), 1521 (m), 1364 (m), 1330 (m), 1244 (s), 1170 (s), 1141 (m), 1097 (w), 1025 (m), 794 (w), 759 (w), 525 (w) cm⁻¹. MS (ESI+ve) *m/z* 401 (³⁵Cl [M+H]⁺, 100%), 403 (³⁷Cl [M+H]⁺, 33%). HRMS (ESI+ve TOF) calcd for C₂₁H₂₆³⁵ClN₄O₂ 401.1736, found 401.1744 ([M+H]⁺).

2-(2-(4-(3-Aminopropoxy)phenyl)-6-chloroimidazo[1,2-a]pyridin-3-yl)-N,N-diethylacetamide (22b)

Following **General Procedure E**, *O*-alkylated phenol (**21b**; 206 mg, 0.40 mmol) was dissolved in CHCl_2 (4.0 mL) and treated with $\text{CF}_3\text{CO}_2\text{H}$ (1.2 mL) to afford the free amine (**22b**; 152 mg, 92%) a pale-yellow foam that collapsed into a translucent gum after preparative TLC plate chromatography. TLC ($\text{CH}_2\text{Cl}_2/\text{MeOH}$ 95:5): $R_f=0.55$. ^1H NMR (400 MHz, DMSO): $\delta=8.51$ (br s, 1H), 7.60 (d, $J=9.6$ Hz, 1H), 7.53 (d, $J=8.8$ Hz, 2H), 7.27 (dd, $J=9.6$, 2.0 Hz, 1H), 7.02 (d, $J=8.8$ Hz, 2H), 4.21 (s, 2H), 4.06 (t, $J=5.6$ Hz, 2H), 3.46 (q, $J=7.2$ Hz, 2H), 3.45–3.34 (m, 4H), 2.75 (t, $J=5.6$ Hz, 2H), 1.83 (quint, $J=5.6$ Hz, 2H), 1.17 (t, $J=7.2$ Hz, 3H), 1.05 (t, $J=7.2$ Hz, 3H). ^{13}C NMR (400 MHz, DMSO): $\delta=167.0$, 158.4, 143.5, 142.2, 129.0, 126.5, 124.7, 123.0, 118.4, 117.1, 116.4, 114.6, 65.5, 63.5, 41.7, 38.0, 31.6, 28.7, 14.2, 13.0. IR (neat) $_{\text{max}}$ 3367 (w), 2968 (w), 2932 (w), 1715 (w), 1632 (s), 1500 (m), 1389 (m), 1331 (m), 1246 (s), 1175 (m), 1141 (m), 1097 (w), 1025 (s), 795 (w), 761 (w), 526 (w) cm^{-1} . MS (ESI+ve) m/z 415 (^{35}Cl $[M+H]^+$, 100%), 417 (^{37}Cl $[M+H]^+$, 33%). HRMS (ESI+ve TOF) calcd for $\text{C}_{22}\text{H}_{28}^{35}\text{ClN}_4\text{O}_2$ 415.1895, found 415.1901 ($[M+H]^+$).

2-(6-Chloro-2-(4-(2-((7-nitrobenzo[c][1,2,5]oxadiazol-4-yl)amino)ethoxy)phenyl)imidazo[1,2-a]pyridin-3-yl)-N,N-diethylacetamide (23a)

Following **General Procedure C**, amine (**22a**; 66 mg, 0.16 mmol) was dissolved in DMF (3.2 mL) followed by sequential addition of DIPEA (30 mg, 0.22 mmol) and NBD-Cl (**14**; 33 mg, 0.16 mmol) to afford the desired fluorescent probe (**23a**; 40 mg, 44%) as a light-brown solid after preparative TLC plate chromatography ($\text{CH}_2\text{Cl}_2/\text{MeOH}$ 98:2). TLC ($\text{CH}_2\text{Cl}_2/\text{MeOH}$ 98:2): $R_f=0.30$. mp = 102–104 °C (decomp). NMR (500 MHz, DMSO): $\delta=9.63$ (br s, 1H), 8.56 (d, $J=9.0$ Hz, 1H), 8.52 (s, 1H), 7.61 (d, $J=9.5$ Hz, 1H), 7.54 (d, $J=9.0$ Hz, 2H), 7.29 (dd, $J=9.5$, 2.0 Hz, 1H), 7.06 (d, $J=9.0$ Hz, 2H), 6.58 (d, $J=9.0$ Hz, 1H), 4.36 (t, $J=6.0$ Hz, 2H), 4.20 (s, 2H), 3.92 (s, 2H), 3.45 (q, $J=7.0$ Hz, 2H), 3.31 (q, $J=7.0$ Hz, 2H), 1.17 (t, $J=7.0$ Hz, 3H), 1.07 (t, $J=7.0$ Hz, 3H). ^{13}C NMR (500 MHz, DMSO): $\delta=167.0$, 157.9, 145.3, 144.5, 144.1, 143.3, 142.2, 137.9, 129.0, 127.0, 124.8, 123.0, 121.2, 118.5, 117.2, 116.5, 114.7, 99.7, 65.6, 43.0, 41.7, 40.1, 28.7, 14.2, 13.1. IR (neat) $_{\text{max}}$ 3243 (w), 2976 (w), 1636 (m), 1583 (s), 1499 (s), 1444 (s), 1326 (m), 1292 (s), 1250 (s), 1128 (m), 1026 (m), 994 (m), 799 (m), 739 (m), 595 (m), 523 (m) cm^{-1} . MS (ESI+ve) m/z 564 (^{35}Cl $[M+H]^+$, 100%), 566 (^{37}Cl $[M+H]^+$, 33%); (ESI–ve) m/z 562 (^{35}Cl $[M-H]^-$, 100%), 564 (^{37}Cl $[M-H]^-$, 33%). HRMS (ESI+ve TOF) calcd for $\text{C}_{27}\text{H}_{27}^{35}\text{ClN}_7\text{O}_5$ 564.1757, found 564.1762 ($[M+H]^+$).

2-(6-Chloro-2-(4-(3-((7-nitrobenzo[c][1,2,5]oxadiazol-4-yl)amino)propoxy)phenyl)imidazo[1,2-a]pyridin-3-yl)-N,N-diethylacetamide (23b)

Following **General Procedure C**, amine (**22b**; 80 mg, 0.19 mmol) was dissolved in DMF (3.8 mL) followed by sequential addition of DIPEA (34 mg, 0.27 mmol) and NBD-Cl (**14**; 38 mg, 0.19 mmol) to afford the desired fluorescent probe (**23b**; 46 mg, 42%) as a light-brown solid after preparative TLC plate chromatography ($\text{CH}_2\text{Cl}_2/\text{MeOH}$ 98:2). TLC ($\text{CH}_2\text{Cl}_2/\text{MeOH}$ 98:2): $R_f=0.41$. mp = 105–107 °C (decomp). NMR (500 MHz, DMSO): $\delta=9.58$ (br s, 1H), 8.52 (s, 1H), 8.49 (d, $J=9.0$ Hz, 1H), 7.60 (d, $J=9.5$ Hz, 1H), 7.53 (d, $J=9.0$ Hz, 2H), 7.28 (dd, $J=9.5$, 2.0 Hz, 1H), 7.04 (d, $J=9.0$ Hz, 2H), 6.45 (d, $J=9.0$ Hz, 1H), 4.20 (s, 2H), 4.15 (t, $J=6.0$ Hz, 2H), 3.67 (br s, 2H), 3.44 (q, $J=7.0$ Hz, 2H), 3.32 (q, $J=7.0$ Hz, 2H), 2.17 (quint, $J=6.0$ Hz, 2H), 1.16 (t, $J=7.0$ Hz, 3H), 1.06 (t, $J=7.0$ Hz, 3H). ^{13}C NMR (500 MHz, DMSO): $\delta=167.0$, 158.2, 145.2, 144.5, 144.2, 143.4, 142.2, 137.9, 129.0, 126.7, 124.7, 123.0, 120.7, 118.4, 117.1, 116.4,

114.6, 99.2, 65.1, 41.7, 40.4, 40.1, 28.7, 27.5, 14.2, 13.1. IR (neat) $_{\text{max}}$ 3231 (w), 2967 (w), 1632 (m), 1582 (s), 1493 (s), 1464 (m), 1344 (s), 1284 (s), 1240 (m), 1136 (s), 1027 (m), 1009 (m), 802 (m), 740 (w), 596 (m), 525 (m) cm^{-1} . MS (ESI+ve) m/z 578 (^{35}Cl $[M+H]^+$, 100%), 580 (^{37}Cl $[M+H]^+$, 33%); (ESI–ve) m/z 576 (^{35}Cl $[M-H]^-$, 100%), 578 (^{37}Cl $[M-H]^-$, 33%). HRMS (ESI+ve TOF) calcd for $\text{C}_{28}\text{H}_{29}^{35}\text{ClN}_7\text{O}_5$ 578.1913, found 578.1919 ($[M+H]^+$).

2-(6-Chloro-2-(4-((7-nitrobenzo[c][1,2,5]oxadiazol-4-yl)oxy)phenyl)imidazo[1,2-a]pyridin-3-yl)-N,N-diethylacetamide (24)

The phenol (**19**; 175 mg, 0.49 mmol) was dissolved in DMF (4 mL) with magnetic stirring. The solution was brought to 0 °C (ice bath) followed by sequential dropwise addition of DIPEA (256 μL , 1.47 mmol) and a solution of NBD-Cl (**14**; 98 mg, 0.49 mmol) in DMF (1.0 mL) under a flow of N_2 gas. The reaction vessel was then sealed and allowed to warm to RT and stirring was continued for 18 h under N_2 in the dark. The solution was partitioned between CHCl_3 (100 mL) and H_2O (100 mL). The aqueous phase was separated and extracted with CHCl_3 (3 \times 50 mL). The combined organic extracts were washed with H_2O (2 \times 100 mL), brine (2 \times 100 mL), dried (Na_2SO_4), filtered, and concentrated. The residue was subjected to flash chromatography over SiO_2 gel ($\text{CH}_2\text{Cl}_2/\text{MeOH}$ 95:5) to afford the fluorescent probe (**24**; 110 mg, 43%) as a brown solid. TLC ($\text{CH}_2\text{Cl}_2/\text{MeOH}$ 90:10): $R_f=0.65$. mp = 98–100 °C (decomp). ^1H NMR (400 MHz, DMSO): $\delta=8.67$ (d, $J=8.4$ Hz, 1H), 8.58 (dd, $J=2.0$, 0.8 Hz, 1H), 7.82 (d, $J=8.8$ Hz, 2H), 7.67 (dd, $J=9.6$, 0.8 Hz, 1H), 7.54 (d, $J=8.8$ Hz, 2H), 7.35 (dd, $J=9.6$, 2.0 Hz, 1H), 6.84 (d, $J=8.4$ Hz, 1H), 4.31 (s, 2H), 3.48 (q, $J=7.2$ Hz, 2H), 3.33 (q, $J=7.2$ Hz, 2H), 1.20 (t, $J=7.2$ Hz, 3H), 1.07 (t, $J=7.2$ Hz, 3H). ^{13}C NMR (400 MHz, DMSO): $\delta=166.9$, 153.1, 152.5, 145.4, 144.4, 142.4, 142.3, 135.5, 132.9, 130.4, 129.9, 125.3, 123.2, 121.0, 118.8, 117.6, 117.5, 110.0, 41.7, 40.2, 28.7, 14.2, 13.1. IR (neat) $_{\text{max}}$ 3404 (w), 2990 (w), 1632 (s), 1537 (s), 1521 (s), 1500 (s), 1450 (s), 1267 (s), 1257 (s), 1203 (s), 1088 (s), 1025 (s), 996 (s), 803 (s) cm^{-1} . MS (ESI+ve) m/z 521 (^{35}Cl $[M+H]^+$, 100%), 523 (^{37}Cl $[M+H]^+$, 100%); HRMS (ESI+ve TOF) calcd for $\text{C}_{25}\text{H}_{21}^{35}\text{ClN}_6\text{O}_5$ 521.1335, found 521.1340 ($[M+H]^+$).

Biological studies

Animals. Male Sprague-Dawley rats and C57BL/6J mice were purchased from Japan SLC (Shizuoka, Japan), kept in temperature-controlled environment with a 12 h light-dark cycle, and fed a standard diet (MB-1/Funabashi Farm, Chiba, Japan). Animals were treated and handled according to the recommendations specified by the Committee for the Care and Use of Laboratory Animals of the National Institutes for Quantum and Radiological Science and Technology (QST) and Animal Research: Reporting of In Vivo Experiments (ARRIVE) guidelines. All animal experiments were approved (approved number: 16-1006) by the committee of QST. For *in vitro* fluorescence staining, six-months-old mice anesthetized with 1.5% (v/v) isoflurane were injected with 2 μL of LSP in saline (2 mg/mL) into striatum (Interaural 3.82 mm, Lateral 2.0 mm, Depth 2.5 mm) of right hemisphere *via* glass capillary.

In vitro binding assay. Four rats (8–10 weeks old) were sacrificed by cervical dislocation under anesthesia (5% isoflurane in air). The brains were rapidly removed and homogenized in ten volumes of 50 mM Tris-HCl (pH 7.4) containing 320 mM sucrose (Tris buffer) using a Silent Crusher S homogenizer (Heidolph Instruments, Schwabach, Germany). The homogenate was centrifuged in a polypropylene tube at 800g for 10 min at 4 °C. The supernatant was collected and then centrifuged at 9000g for 10 min at 4 °C using an Optima-TLX (Beckman Coulter, Brea, CA). After discarding the supernatant, the pellet was suspended in Tris-buffer and

centrifuged at 9000g for 10 min at 4 °C. Subsequently, the resulting pellet was resuspended in Tris buffer and centrifuged at 12000g for 10 min at 4 °C. Finally, the crude mitochondrial pellet was resuspended in 50 mM Tris·HCl buffer containing 120 mM NaCl, 2 mM KCl, 1 mM MgCl₂, and 1 mM CaCl₂ (Wash-buffer) at a concentration of 100 µg original wet tissue /mL and used for binding assays. Each crude mitochondrial preparation of 0.1 mL was incubated with [¹¹C]PK11195 (final concentration: 3.4 ± 2.6 nM) and various concentrations of test compounds (**15 a–15 d**, **17**, **23 a**, **23 b**, **24**, and PK11195) in a final volume of 1 mL buffer. These mixtures were incubated for 30 min at room temperature. The bound and free radioactivities were separated by vacuum filtration through 0.3% polyethylenimine-pretreated Whatman GF/C glass fiber filters using a cell harvester (M-24, Brandel, Gaithersburg, MD), followed by three washes with prechilled wash buffer. The radioactivity of filters containing the bound [¹¹C]PK11195 was counted with a 2480 Wizard² autogamma scintillation counter (PerkinElmer). Nonspecific binding was determined in the presence of PK11195 (10 µM). All assays were performed in duplicate. Specific binding at each compound concentration was calculated as a percentage in relation to the control specific binding, and which were converted to probit values to determine the IC₅₀ of each compound. The IC₅₀ value was further converted to K_i according to the Cheng–Prusoff equation.^[41] In that equation, the dissociation constant of [¹¹C]PK11195 was referred from a previous paper.^[42]

In vitro fluorescence staining. Mice were deeply anesthetized and sacrificed by cervical dislocation, and brains were subsequently dissected and frozen in OCT compound (SaKuRa). Fixed frozen sections (20-µm thick) were prepared by cryostat and incubated in 50 mM Tris·HCl buffer containing 0.001% (w/v) of ligand at room temperature for 30 min. The brain samples were rinsed with 50 mM Tris·HCl twice for 2 min, dipped into distilled water for 10 s, and mounted in nonfluorescent mounting medium (VECTASHIELD, Vector Laboratories). Fluorescence images were captured using a DM4000 microscope equipped with filter cube for FITC (excitation filter: band-pass at 460–500 nm; suppression filter: band-pass at 512–542 nm) and Rhodamine (excitation filter: band-pass at 515–560 nm; suppression filter: long-pass at 590 nm), and a BZ-X710 fluorescence microscope equipped with filter cube for FITC (excitation filter: band-pass at 450–490 nm; suppression filter: band-pass at 500–550 nm). Sections labeled with ligands were fixed in 4% PFA in PBS for overnight at 4 °C and autoclaved for antigen retrieval and immunostained with anti-TSPO antibody (1:1000, ab109497, Abcam). Immunolabelling was then examined using DM4000 and BZ-X710.

Acknowledgements

HW thanks Ministry of Research and Technology (Indonesia) for PhD scholarship funding under Research and Innovation in Science and Technology Project (RISET-Pro) no. 8245-ID.

Conflict of Interest

The authors declare no conflict of interest.

Keywords: biological evaluations · fluorescent probes · imaging · neurodegenerative diseases · translocator protein

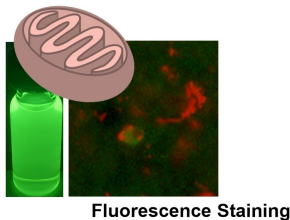
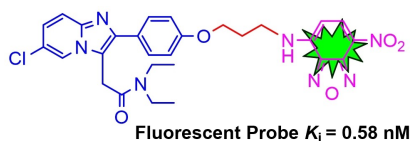
- [1] G. J. Liu, R. J. Middleton, C. R. Hatty, W. W. Kam, R. Chan, T. Pham, M. Harrison-Brown, E. Dodson, K. Veale, R. B. Banati, *Brain Pathol.* **2014**, *24*, 631–653.
- [2] G. Scott, M. Mahmud, D. R. Owen, M. R. Johnson, *Seizure* **2017**, *44*, 42–47.
- [3] M. K. Chen, T. R. Guilarte, *Pharmacol. Ther.* **2008**, *118*, 1–17.
- [4] L. Biswas, F. Farhan, J. Reilly, C. Bartholomew, X. Shu, *Int. J. Mol. Sci.* **2018**, *19*, 1–16.
- [5] B. Largeau, A. C. Dupont, D. Guilloleau, M. J. Santiago-Ribeiro, N. Arlicot, *Contrast Media Mol. Imaging.* **2017**, *2017*, 1–17.
- [6] F. Roncaroli, Z. Su, K. Herholz, A. Gerhard, F. E. Turkheimer, *Clin. Transl. Imaging* **2016**, *4*, 145–156.
- [7] M. N. Tantawy, H. Charles Manning, T. E. Peterson, D. C. Colvin, J. C. Gore, W. Lu, Z. Chen, C. Chad Quarles, *Mol. Imaging Biol.* **2018**, *20*, 200–204.
- [8] M. A. Ostuni, R. Ducroc, G. Peranzi, M. C. Tonon, V. Papadopoulos, J. J. Lacapere, *Biol. Cell* **2007**, *99*, 639–647.
- [9] T. Zhou, Y. Dang, Y. H. Zheng, *J. Virol.* **2014**, *88*, 3474–3484.
- [10] N. H. Bhoola, Z. Mbita, R. Hull, Z. Dlamini, *Int. J. Mol. Sci.* **2018**, *19*, 1–23.
- [11] L. Vivash, T. J. O'Brien, *J. Nucl. Med.* **2016**, *57*, 165–168.
- [12] M. Perrone, B. S. Moon, H. S. Park, V. Laquintana, J. H. Jung, A. Cutrignelli, A. Lopodota, M. Franco, S. E. Kim, B. C. Lee, N. Denora, *Sci. Rep.* **2016**, *6*, 1–13.
- [13] Y. Cui, T. Takashima, M. Takashima-Hirano, Y. Wada, M. Shukuri, Y. Tamura, H. Doi, H. Onoe, Y. Kataoka, Y. Watanabe, *J. Nucl. Med.* **2009**, *50*, 1904–1911.
- [14] F. Mattner, A. Katsifis, M. Staykova, P. Ballantyne, D. O. Willenborg, *Eur. J. Nucl. Med. Mol. Imaging* **2005**, *32*, 557–563.
- [15] K. Yanamoto, K. Kumata, T. Yamasaki, C. Odawara, K. Kawamura, J. Yui, A. Hatori, K. Suzuki, M. R. Zhang, *Bioorg. Med. Chem. Lett.* **2009**, *19*, 1707–1710.
- [16] K. Kumata, Y. Zhang, M. Fujinaga, T. Ohkubo, W. Mori, T. Yamasaki, M. Hanyu, L. Xie, A. Hatori, M. R. Zhang, *Bioorg. Med. Chem.* **2018**, *26*, 4817–4822.
- [17] L. P. Dickstein, S. S. Zoghbi, Y. Fujimura, M. Imaizumi, Y. Zhang, V. W. Pike, R. B. Innis, M. Fujita, *Eur. J. Nucl. Med. Mol. Imaging* **2011**, *38*, 352–357.
- [18] L. Vomacka, N. L. Albert, S. Lindner, M. Unterrainer, C. Mahler, M. Brendel, L. Ermoschkin, A. Gosewisch, A. Brunegraf, C. Buckley, T. Kumpfel, R. Rupprecht, S. Ziegler, M. Kerschensteiner, P. Bartenstein, G. Boning, *EJNMMI. Res.* **2017**, *7*, 1–9.
- [19] J. Zhao, J. Chen, S. Ma, Q. Liu, L. Huang, X. Chen, K. Lou, W. Wang, *Acta Pharm. Sin.* **2018**, *8*, 320–338.
- [20] Y. Sun, X. Zeng, Y. Xiao, C. Liu, H. Zhu, H. Zhou, Z. Chen, F. Xu, J. Wang, M. Zhu, J. Wu, M. Tian, H. Zhang, Z. Deng, Z. Cheng, X. Hong, *Chem. Sci.* **2018**, *9*, 2092–2097.
- [21] L. Bu, B. Shen, Z. Cheng, *Adv. Drug Delivery Rev.* **2014**, *76*, 21–38.
- [22] L. Sun, J. Ding, W. Xing, Y. Gai, J. Sheng, D. Zeng, *Bioconjugate Chem.* **2016**, *27*, 1200–1204.
- [23] A. Trapani, C. Palazzo, M. de Candia, F. M. Lasorsa, G. Trapani, *Bioconjugate Chem.* **2013**, *24*, 1415–1428.
- [24] S. Taliani, F. Simorini, F. Sergianni, C. L. Motta, F. D. Settimo, B. Cosimelli, E. Abignente, G. Greco, E. Novellino, L. Rossi, V. Gremigni, F. Spinneti, B. Chelli, C. Martini, *J. Med. Chem.* **2007**, *50*, 404–407.
- [25] V. Laquintana, N. Denora, A. Lopodota, H. Suzuki, M. Sawada, M. Serra, G. Biggio, A. Latrofa, G. Trapani, G. Liso, *Bioconjugate Chem.* **2007**, *18*, 1397–1407.
- [26] C. Milite, E. Barresi, E. Da Pozzo, B. Costa, M. Viviano, A. Porta, A. Messere, G. Sbardella, F. Da Settimo, E. Novellino, S. Cosconati, S. Castellano, S. Taliani, C. Martini, *J. Med. Chem.* **2017**, *60*, 7897–7909.
- [27] J. Li, J. A. Smith, E. S. Dawson, A. Fu, M. L. Nickels, M. L. Schulte, H. C. Manning, *Bioconjugate Chem.* **2017**, *28*, 1016–1023.
- [28] N. Denora, V. Laquintana, A. Trapani, H. Suzuki, M. Sawada, G. Trapani, *Pharm. Res.* **2011**, *28*, 2820–2832.
- [29] M. Bai, M. B. Rone, V. Papadopoulos, D. J. Bornhop, *Bioconjugate Chem.* **2007**, *18*, 2018–2023.
- [30] M. Bai, S. K. Wyatt, Z. Han, V. Papadopoulos, D. J. Bornhop, *Bioconjugate Chem.* **2007**, *18*, 1118–1122.
- [31] S. K. Wyatt, H. C. Manning, M. Bai, S. N. Bailey, P. Gallant, G. Ma, L. McIntosh, D. J. Bornhop, *Mol. Imaging Biol.* **2010**, *12*, 349–358.
- [32] A. Cutrignelli, N. Denora, M. Franco, E. Kim Sang, V. Laquintana, B.-C. Lee, S. H. Lee, A. A. Lopodota (Seoul Nat Univ R&Db Foundation) WO2019143016A1, **2019**.
- [33] T. P. Homes, *PhD Thesis*, University of Wollongong, Australia **2007**.

- [34] C. J. R. Fookes, T. Q. Pham, F. Mattner, I. Greguric, C. Loc'h, X. Liu, P. Berghofer, R. Shepherd, M. C. Gregoire, A. Katsifis, *J. Med. Chem.* **2008**, *51*, 3700–3712.
- [35] "Application of NBD-Labeled Lipids in Membrane and Cell Biology", S. Haldar A. Chattopadhyay in *Fluorescent Methods To Study Biological Membranes*, (Ed(s): Y. Mély, G. Duporta), Springer, Berlin, **2012**, pp. 37–50.
- [36] M. Amaro, H. A. Filipe, J. P. Prates Ramalho, M. Hof, L. M. Loura, *Phys. Chem. Chem. Phys.* **2016**, *18*, 7042–7054.
- [37] M. Bem, F. Badea, C. Draghici, M. T. Caproiu, M. Vasilescu, M. Voicescu, A. Beteringhe, A. Caragheorgheopol, M. Maganu, T. Constantinescu, A. T. Balaban, *Arkivoc* **2007**, *13*, 87–104.
- [38] A. Hatori, J. Yui, T. Yamasaki, L. Xie, K. Kumata, M. Fujinaga, Y. Yoshida, M. Ogawa, N. Nengaki, K. Kawamura, T. Fukumura, M. R. Zhang, *PLoS One* **2012**, *7*, 1–8.
- [39] J. Lange, J. K. Wojciechowska, K. Wejroch, S. Rump, *Acta Pol. Pharm.* **2001**, *58*, 43–52.
- [40] Y. Liu, Q. Qiao, M. Zhao, W. Yin, L. Miao, L. Wang, Z. Xu, *Dyes Pigm.* **2016**, *133*, 339–344.
- [41] Y. C. Cheng, W. H. Prusoff, *Biochem. Pharmacol.* **1993**, *22*, 3099–3108.
- [42] A. Kita, H. Kohayakawa, T. Kinoshita, Y. Ochi, K. Nakamichi, S. Kurumiya, K. Furukawa, M. Oka, *Br. J. Pharmacol.* **2004**, *142*, 1059–1072.

Manuscript received: December 23, 2020
Revised manuscript received: February 22, 2021
Accepted manuscript online: February 25, 2021
Version of record online: ■■■, ■■■■

FULL PAPERS

Towards monitoring neuroinflammation and -degeneration: A series of TSPO-targeted probes based on 6-chloro-2-phenylimidazo[1,2-a]pyridine-3-yl acetamide ligands with a NBD fluorophore has been designed and synthesised. Their efficacy was assessed in a competitive binding assay on TSPO receptors against [¹¹C]PK11195. The probe with the most potential can be considered to be eligible for investigating activated microglia.



Dr. H. Wongso, Dr. T. Yamasaki, Dr. K. Kumata, Prof. M. Ono, Prof. M. Higuchi, Prof. M.-R. Zhang, Prof. M. J. Fulham, Prof. A. Katsifis*, Prof. P. A. Keller**

1 – 16

Design, Synthesis, and Biological Evaluation of Novel Fluorescent Probes Targeting the 18-kDa Translocator Protein

